A COMPILATION OF RATE PARAMETERS OF WATER-MINERAL INTERACTION KINETICS FOR APPLICATION TO GEOCHEMICAL MODELING

U.S. GEOLOGICAL SURVEY

OPEN FILE REPORT 2004-1068

U.S. Department of the Interior
U.S. Geological Survey

A COMPILATION OF RATE PARAMETERS OF WATER-MINERAL INTERACTION KINETICS FOR APPLICATION TO GEOCHEMICAL MODELING

James L. Palandri and Yousif K. Kharaka

U.S. GEOLOGICAL SURVEY

Menlo Park, California
March 2004

U.S. DEPARTMENT OF THE INTERIOR
GALE NORTON, Secretary

U.S. GEOLOGICAL SURVEY
CHARLES GROAT, Director

Any use of trade, firm, or product names is for descriptive purposes only and does not imply endorsement by the U.S. Government.

CONTENTS

LIST OF FIGURES

LIST OF TABLES

Conversion Factors

Multiply	By	To obtain
meter (m)	39.37	inch (in.)
meter (m)	3.281	foot (ft)
meter (m)	1.094	yard (yd)
square meter (m2)	10.76	square foot (ft2)
square meter (m2)	1549.44	square inch (in2)
kilogram (kg)	35.27	ounce, avoirdupois (oz)
kilogram (kg)	2.205	pound avoirdupois (lb)
joule (J)	0.0000002	kilowatt-hour (kWh)

Temperature in degrees Celsius (°C) may be converted to degrees Fahrenheit (°F) as follows:

$$°F = (1.8 × °C) + 32$$

ABSTRACT

Geochemical reaction path modeling is useful for rapidly assessing the extent of water-aqueous-gas interactions both in natural systems and in industrial processes. Modeling of some systems, such as those at low temperature with relatively high hydrologic flow rates, or those perturbed by the subsurface injection of industrial waste such as CO_2 or H_2S, must account for the relatively slow kinetics of mineral-gas-water interactions. We have therefore compiled parameters conforming to a general Arrhenius-type rate equation, for over 70 minerals, including phases from all the major classes of silicates, most carbonates, and many other non-silicates. The compiled dissolution rate constants range from -0.21 log moles m^{-2} s^{-1} for halite, to -17.44 log moles m^{-2} s-1 for kyanite, for conditions far from equilibrium, at 25 °C, and pH near neutral. These data have been added to a computer code that simulates an infinitely well-stirred batch reactor, allowing computation of mass transfer as a function of time. Actual equilibration rates are expected to be much slower than those predicted by the selected computer code, primarily because actual geochemical processes commonly involve flow through porous or fractured media, wherein the development of concentration gradients in the aqueous phase near mineral surfaces, which results in decreased absolute chemical affinity and slower reaction rates. Further differences between observed and computed reaction rates may occur because of variables beyond the scope of most geochemical simulators, such as variation in grain size, aquifer heterogeneity, preferred fluid flow paths, primary and secondary mineral coatings, and secondary minerals that may lead to decreased porosity and clogged pore throats.

1. INTRODUCTION

Equilibrium-based geochemical modeling is a method for predicting the identity and extent of chemical reactions in both geological and industrial processes. The method usually entails computer-aided simultaneous solution of a system of non-linear equations. Given a pressure (P), a temperature (T), and a bulk chemical composition (x), a geochemical modeling program or simulator computes the equilibrium distribution of the chemical components among gaseous, aqueous, or mineral phases. The variables P, T, or x can be changed incrementally over the course of a simulation with equilibrium recomputed at each step, thereby defining a reaction path. Some geochemical simulators, such as GAMSPATH (for a description of GAMSPATH, and comparison of GAMSPATH to other geochemical simulators, see Perkins et al., 1997), require the presence of an aqueous fluid phase and are well suited to simulation of systems at shallow to moderate depth in the Earth's crust, or wherever there is open space that is saturated with water, such as pores or fractures. Water is the medium that allows mass transfer by diffusion or fluid flow, and redistribution of the components via chemical reaction among the gaseous and various mineral phases, and species in the aqueous phase. Considered herein is the quantification of the rates at which these reactions occur.

Local non-redox chemical equilibria among fluids, gases, and alteration minerals is a valid assumption in many volcanic-hosted hydrothermal systems (Arnórsson, 1983; Arnórsson et al., 1983; Giggenbach, 1980; Giggenbach, 1981; Pang and Reed, 1998; Reed, 1982; Reed, 1997;

Reed, 1998; Reed and Spycher, 1984), and in many sedimentary systems with low fluid flow rates at temperatures as low as 75-80 °C (Bazin et al., 1997a; Bazin et al., 1997b; Palandri and Reed, 2001). In other systems, equilibrium with an alteration mineral assemblage cannot always be assumed, especially in systems where low temperature leads to slow rates of chemical reaction, or if there exists a perturbation away from equilibrium, e.g. relatively fast hydrologic flow rates from one lithologic regime into another. It is important to recognize that equilibrium between aqueous fluid and primary minerals is commonly lacking, and in some cases cannot be attained, e.g. anorthite or forsterite at T and P of H_2O liquid-vapor saturation. Further, equilibrium between aqueous fluid and secondary minerals containing redox elements such as Fe and S generally requires higher temperatures than for those minerals containing only non-redox elements (other than oxygen).

For many geologic systems it is desirable to know the length of time required for a system to equilibrate with respect to alteration minerals, and perhaps more importantly, the rate of dissolution of primary minerals. An illustrative example is the geologic sequestration of carbon dioxide (CO_2) from anthropogenic sources, such as fossil fuel-fired electrical power plants, is injected into depleted oil or gas reservoirs, coal seams, or deep saline aquifers. As a result of CO_2 injection, these systems are perturbed far from equilibrium, and will require some length of time to re-equilibrate with alteration minerals, due to the relatively slow kinetics of mineral-CO_2-water interactions at aquifer temperatures and pressures. While dissolution of supercritical CO_2 into aquifer fluids is expected to be kinetically rapid, the rate at which dissolved CO_2 reacts with primary minerals, and the rates at which secondary minerals precipitate are much slower (Gunter et al., 1997).

To model systems where the time dependence of geochemical reactions is of critical importance, there is a need to quantify rates of mineral dissolution and precipitation, and to a lesser extent, of aqueous speciation. Therefore, we compiled directly or determined using regression and curve-fitting, the parameters conforming to a general, Arrhenius-type rate equation for over 70 minerals, including most of the rock-forming minerals. For a few minerals, we have also compiled more specialized rate equations and parameters, where some workers have clearly shown that those equations provide a better fit to experimental data, e.g. quartz (Dove, 1994; Dove, 1999; Dove and Nix, 1997) and barite (Dove and Czank, 1995). The rate parameters compiled herein are for surface controlled reactions at conditions that are far from equilibrium, rather than diffusion controlled reactions. This compilation does not contain rate parameters for aqueous speciation.

2. METHODS

2.1 Rate Equations

Any rate equation that is to be used in geochemical computer modeling must contain only parameters that are available during program execution as variables or constants. The general rate equation and rate parameters compiled herein are compiled specifically for the program GAMSPATH (Perkins et al., 1997), which uses a general, semi-empirical rate equation to which experimental rate data for many minerals can be reasonably well fit. A general form of the

equation for a single reaction mechanism modified from Lasaga and co-workers (1984; 1995; 1998) is given by

$$\frac{dm}{dt} = -SA \cdot A e^{-E/RT} f(a_i) g(\Delta G_r)$$

(1)

and for multiple mechanisms

$$\frac{dm}{dt} = -SA \cdot \sum_j [A_j e^{-E_j/RT} f_j(a_{i,j}) g_j(\Delta G_r)]$$

(2)

The rate, dm/dt, is in units of mol s^{-1}. The surface area is represented by SA (m^2), A is the Arrhenius pre-exponential factor (mol m^{-2} s^{-1}), E is the activation energy (J mol^{-1}), T is the temperature (K), and R is the gas constant.

The dimensionless terms $f_j(a_{i,j})$ are functions of the activity of the ith aqueous species participating in the jth reaction mechanism. The function for a single mechanism is commonly expressed as the product of species activities

$$f(a_i) = \prod_i a_i^{n_i}$$

(3a)

where the exponents n_i represent the reaction order with respect to species a_i (Lasaga, 1995; Lasaga, 1998; Lasaga et al., 1994; Oelkers et al., 1994). For example, the expression

$$f(a_i) = a_{H^+}^{-0.5} a_{Fe^{3+}}^{0.5}$$

(3b)

is for one of the reaction mechanisms for pyrite (McKibben and Barnes, 1986), discussed further, below. Positive and negative exponents denote catalysts and inhibitors respectively, except in the case of hydroxide-catalyzed mechanisms (as above in eqn. (3b)), which are quantified in terms of a_{H^+} raised to a negative exponent (recall that for aqueous fluids, $a_{H^+} a_{OH^-} = 10^{-14}$) to simplify calculations. It is important to recognize that eqn. (3b) becomes problematic when a_i is zero and n_i is positive, because the rate becomes zero, which cannot occur for some mechanisms, or if a_i is zero and n_i is negative, because a numerical singularity occurs. These problems can be avoided by defining f with adsorption isotherms (Blum and Lasaga, 1991; Brady, 1992; Casey and Sposito, 1992; Furrer and Stumm, 1986; Gautier et al., 1994; Kline and Fogler, 1981; Pokrovsky and Schott, 1999; Stillings and Brantley, 1995), which have the form

$$f(a_i) = 1 + k_{ad}\left(\frac{K_{Na^+}a_{Na^+}}{1 + K_{Na^+}a_{Na^+}}\right)$$

(3c)

This expression is an example is an isotherm of the Langmuir type for quartz (Dove, 1994; Dove, 1999; Dove and Nix, 1997), where K_{Na^+} is the adsorption coefficient for Na^+, and k_{ad} is a constant factor by which the overall rate constant in adjusted. The sign of k_{ad} is positive for catalysts and negative for inhibitors. GAMSPATH currently does not implement adsorption isotherms, and uses the form as in eqns. (3a) and (3b).

The dimensionless term $g(\Delta G_r)$ is a function of the chemical affinity to account for slowing of reaction rates as equilibrium is approached, and may be expressed as (Lasaga, 1995; Lasaga, 1998; Lasaga et al., 1994; Oelkers et al., 1994):

$$g(\Delta G_r) = (1 - \Omega^{p_i})^{q_i} = (1 - \left[\frac{Q}{K}\right]^{p_i})^{q_i}$$

(4)

Omega ($\Omega = Q/K$) is the mineral saturation index where Q is the activity product, and K is the equilibrium constant. The parameters p_i and q_i are empirical and dimensionless, although p_i can be predicted from transition state theory if the details of the reaction mechanism are known (Lasaga, 1995; Lasaga, 1998); p_i and q_i have been quantified for only a few minerals (discussed below), and for those minerals only for a single mechanism; in all other cases, the default values for p_i and q_i are to a first approximation, unity. Uncertainties in values for p_i and q_i are currently the source of much uncertainty in the length of time to system equilibration computed in models of water-rock interaction. It has been observed for some minerals that there is an apparent significant slowing of the dissolution rate at low degrees of undersaturation (Lasaga, 1995; Lasaga, 1998; Lasaga et al., 1994). For example gibbsite (Nagy and Lasaga, 1992) and albite (Burch et al., 1993), show a stepped shape in a plot of dissolution rate versus chemical affinity.

The overall equation implemented in GAMSPATH is a sum of multiple mechanisms

$$\frac{dm}{dt} = -SA\sum_i [A_i e^{-E_i/RT} \prod_j a_{i,j}^{n_{i,j}} (1 - \Omega^{p_i})^{q_i}]$$

(5)

but recast in terms of rate constants at 298.15 K (25 °C) and pH = 0 to facilitate comparison of various rates among minerals at near-surface T

$$\frac{dm}{dt} = -SA\sum_i [k_i^{298.15K} e^{\frac{-E_i}{R}\left(\frac{1}{T} - \frac{1}{298.15K}\right)} \prod_j a_{i,j}^{n_{i,j}} (1 - \Omega^{p_i})^{q_i}]$$

(6)

4

In general, the most well-studied mechanisms are those in pure H_2O (neutral pH), and those catalyzed by H^+ (acid) and OH^- (base). For many minerals, the full equation includes a term for each of these three mechanisms:

$$\frac{dm}{dt} = -SA \begin{bmatrix} k_{acid}^{298.15K} e^{\frac{-E_{acid}}{R}\left(\frac{1}{T} - \frac{1}{298.15K}\right)} a_{H^+}^{n_1} (1-\Omega^{p_1})^{q_1} \\[2ex] + k_{neutral}^{298.15K} e^{\frac{-E_{neut}}{R}\left(\frac{1}{T} - \frac{1}{298.15K}\right)} (1-\Omega^{p_2})^{q_2} \\[2ex] + k_{base}^{298.15K} e^{\frac{-E_{base}}{R}\left(\frac{1}{T} - \frac{1}{298.15K}\right)} a_{H^+}^{n_3} (1-\Omega^{p_3})^{q_3} \end{bmatrix} \qquad (7)$$

The OH^--catalyzed mechanism in eqn. (7) uses the activity of H^+ raised to a reaction order with negative sign, to simplify data reduction. Additional terms are added to or removed from eqn. (7) to account for other mechanisms or the absence of data. Other mechanisms include those catalyzed by HCO_3^-, (especially the carbonate minerals, which are quantified in terms of either HCO_3^- or P_{CO2}), Fe^{3+} (pyrite, pyrrhotite), and O_2 (pyrite). In the case of pyrite and pyrrhotite, the OH^--catalyzed mechanism is apparently slowed by presence of Fe^{3+}. This effect is accounted for by substituting a term in the form of eqn. (3b) for the H^+ activity and reaction order in the third term in eqn. (7). It should be recognized that although the pyrite dissolution rates were measured at low pH, the reaction order with respect to H^+ is negative, i.e. the reaction is OH^--catalyzed.

Precipitation rate data do not exist for most minerals, because in mineral precipitation experiments, undesired metastable reaction products usually precipitate instead of the desired mineral, especially far from equilibrium at high degrees of super-saturation. One example of this behavior is the precipitation of amorphous silica from fluids that are grossly supersaturated with respect to quartz. Further, quartz precipitation is prohibitively slow at low degrees of super-saturation. Therefore, we use the principle of microscopic reversibility (Lasaga, 1998):

$$K_{equilibrium} = \frac{k_{dissolution}}{k_{precipitation}} = \frac{k_+}{k_-} \qquad (8)$$

where the precipitation rate constant can be calculated from the dissolution rate constant and the equilibrium constant. However, it must be recognized that this relation requires that both the forward and backward reactions must both proceed by a single reversible mechanism. Related is the phenomenon of nucleation, where some degree of super-saturation is required for precipitation to proceed (Lebrón and Suárez, 1996; Nordeng and Sibley, 1994; Normand et al., 2002; Reddy, 1986; Schoonen and Barnes, 1991b; Shiraki and Brantley, 1995; Sibley et al., 1987; Steefel and Van Cappellen, 1990); in some cases this can be substantial, as for siderite (Greenberg and Tomson, 1992; Jensen et al., 2002). Nucleation may be either homogeneous,

where nucleation occurs spontaneously in a liquid phase, or heterogeneous, where nucleation of a new phase occurs on the surface of a pre-existing solid phase (Lasaga, 1998). For most minerals, the degree of super-saturation required for homogeneous or heterogeneous nucleation has not been quantified.

For further general discussions of mineral dissolution and precipitation, the reader may wish to consult Anbeek (1993), Bertrand et al. (1994), Brady and Walther (1989), Casey and Sposito (1992), Fleer and Johnston (1986), Gallup (1998), Gérard et al. (1998), Helgeson (1970), Jeschke and Dreybrodt (2002a), Kline and Fogler (1981), Lasaga (1984), Lasaga (1995), Lasaga et al. (1994), Oelkers et al. (1994), Petrovich (1981a), Petrovich (1981b), Schoonen et al. (1998), Steefel and Lasaga (1992), Steefel and Van Cappellen (1990), Sverdrup (1990), Talman and Nesbitt (1988), Tuncay et al. (2002), Wieland et al. (1988), Wood and Walther (1983), Xiao and Lasaga (1994), and Xiao and Lasaga (1996).

2.2 Data Reduction

In this section, we outline a general strategy for the determination of rate parameters conforming to eqn. (6) from experimental data, using the minerals albite and magnesite as examples. Albite is used as an example because it's rate data clearly conform to eqn. (6) in one of its simplified forms, eqn. (7), where rates are controlled by H^+ and OH^- catalysis and temperature. The magnesite example illustrates some problems that may arise if the ability to account for adsorption isotherms is absent: saturation of a mineral surface with a (H^+) catalyst, and the affects of Na^+, which may catalyze or inhibit dissolution depending on pH.

The variables that have the greatest effect on reaction rates are temperature and pH, and fortunately, these variables are almost always reported in by experimentalists. Many minerals show a U-shaped relation (V-shaped on log plots) between dissolution rates and pH, roughly in parallel with their solubilities. For a given temperature, rates are generally slowest at and near the pH where the mineral surface has a net charge of zero, usually within one or two pH units of neutral. At low pH, rates increase with decreasing pH catalyzed by H^+, and at high pH, rates increase with increasing pH, catalyzed by OH^-.

An example of this behavior is shown in Figure 1 for the mineral albite; the data points at 100 to 300 °C are from Hellman (1994a), and at 25 °C, from Chou and Wollast (1985). The curves in Figure 1 are obtained from the data (open symbols) using unweighted non-linear curve fitting (gray curves) and unweighted piecewise linear regression (black curves). Non-linear curve fitting is accomplished by fitting all of the data to a modified version of eqn. (7):

$$\frac{dm}{dt} = -(A_{acid}e^{\frac{-E_{acid}}{RT}}a_{H^+}^{n_1} + A_{neut}e^{\frac{-E_{neut}}{RT}} + A_{base}e^{\frac{-E_{base}}{RT}}a_{H^+}^{n_3}) \qquad (9)$$

The chemical affinity term has been omitted, because we have selected data that is obtained from experiments performed under conditions that are far from equilibrium where Ω approaches zero, and the chemical affinity term approaches unity. The data have been normalized to 1.0 m^2, and the surface area term is omitted as well.

6

Piecewise linear regression is accomplished by first segregating the data into acid, neutral, and basic regions, and fitting the groups of data separately to each of the terms in eqn. (9). For albite the acidic, neutral, and basic regions were selected by Hellman (1994a) to be in the ranges of pH 1.3 to 4.0, 5.6 to 8.2, and 8.6 to 10.3 respectively. For the acidic and basic mechanisms, the equation

$$rate = \frac{dm}{dt} = A_{acid}\, e^{\left(-E_{acid}/RT\right)} a_{H^+}^{n_{H^+}}$$

(10)

can be transformed into the linear relation

$$\log(rate) = \log(A_{acid}) - E_{acid}/(2.3025 RT) - n_{H^+} pH$$

(11)

and for the neutral mechanism, the following relation is used

$$\log(rate) = \log(A_{neutral}) - E_{neutral}/(2.3025 RT)$$

(12)

The black dashed straight lines in Figure 1 show the results for each of the three mechanisms at 100°C, and the black curves represent their sum. It can be seen in Figure 1 that non-linear curve fitting provides a slightly better fit to the data, but for most minerals, lack of agreement in the data among different workers makes this difference negligible.

The results for piecewise linear regression and non-linear regression for albite are shown in Table 1 both in terms of the Arrhenius pre-exponential factor A, and in terms of the rate constant at 25 °C and pH = 0. Our results for piecewise linear regression are in agreement with those of Hellman (1994a) and Chou and Wollast (1985). We recommend application of these parameters only to modeling of systems within the range of conditions under which the parameters were obtained, i.e. from 25 to 300 °C, and $pH_{25°C}$ from 1.3 to 10.3. Albite is one of the few minerals for which p and q have been experimentally determined, but only in alkaline fluids (Alekseyev et al., 1997) at pH = 9; these parameters are also shown in Table 1.

A second illustrative example is for magnesite dissolution at 25 °C (Pokrovsky and Schott, 1999). In this case, magnesite dissolution rates are catalyzed by H^+, and at low pH the mineral surfaces become saturated with H^+ so that further decrease in pH does not cause further increase in dissolution rate. Further, dissolution rates are apparently catalyzed or inhibited by Na^+ depending on pH. Finally, magnesite dissolution rates are independent of OH^-. These experiments were conducted at pH between 0.19 to 10.13 with pH controlled using HCl, NaOH, $NaHCO_3$, and Na_2CO_3, and ionic strength controlled by NaCl. The results are shown graphically in Figure 2.
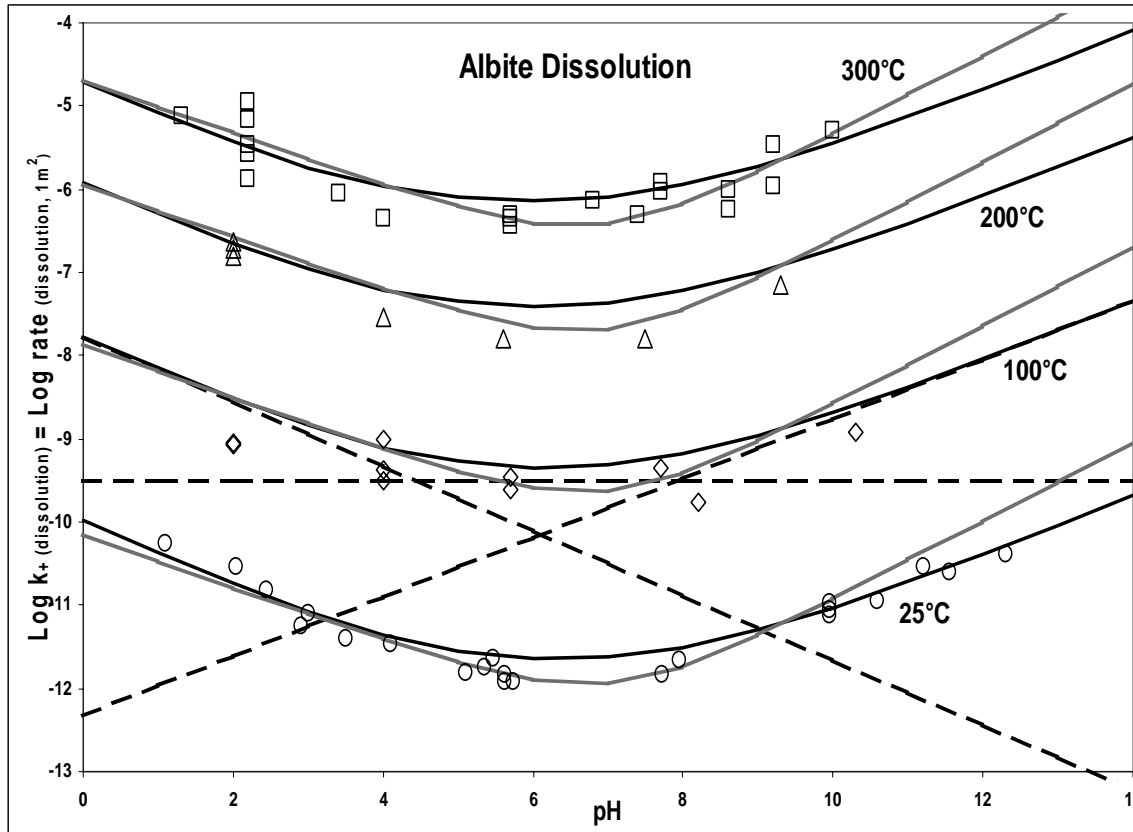
Figure 1. Rates of albite dissolution from 25 to 300 °C and pH from 1.3 to 10.3. Data at 100, 200, and 300 °C (open diamonds, triangles and squares, respectively) from Hellman, 1994, and at 25 °C (open circles) from Chou and Wollast, 1985. Dashed curves: results from non-linear regression. Straight black lines: results from piecewise linear regression of 100 °C data. Black curves: sum of results from piecewise linear regression.

Table 1. Albite Dissolution Rate Parameters.

	Acid Mechanism				Neutral Mechanism			Base Mechanism			
	[a]A	[b]log k	[c]E	[d]n	[a]A	[b]log k	[c]E	[a]A	[b]log k	[c]E	[d]n
Linear Regression	3.23E+01	-9.87	65.0	0.457	1.52E+00	-12.04	69.8	2.96E-05	-16.98	71.0	-0.572
Non-Linear Regression	1.66E+01	-10.16	65.0	0.317	6.66E-02	-12.56	65.0	1.11E-04	-15.60	66.5	-0.471
	p	*q*			*p*	*q*		*p*	*q*		
[e]Chemical Affinity	--	--			--	--		0.76	90.0		

a. Arrhenius pre-exponential factor A, mole m^{-2} s^{-1} for use with equation (5).
b. Log rate constant k computed from A and E, 25°C, pH=0, log moles m^{-2} s^{-1} for use with equation (6).
c. Arrhenius activation energy E, kJ $mole^{-1}$.
d. Reaction order n with respect to H^+.
e. Chemical affinity parameters *p* and *q* default to unity if not specified.

8

In the pH range of 0 to ~3, there is only a minimal dependence of rates on pH, the reaction order with respect to activity of H^+ is small, and increased H^+ activity leads to only a small increase in rates (Figure 2, open squares). This behavior results from the saturation of reactive surface sites with H^+, and can be described using adsorption isotherms (Pokrovsky and Schott, 1999). In the pH range of 3 to 5, faster rates (Fig. 2, open diamonds) apparently result from catalysis by Na^+ at ionic strength 0.1 to 0.5, as compared with slower rates in experiments with low Na^+ concentration (Fig. 2, open triangles) at ionic strength ≤0.1; this behavior can be described using adsorption isotherms for Na^+. Between pH values of 5 and 8, there is minimal dependence on the activity of H^+ or Na^+ (Fig. 2, open triangles) over the entire range of ionic strength from 0.01 to 0.5. At pH greater than 8, Na^+ apparently inhibits reaction rates (Fig. 2, open circles) at ionic strength from 0.004 to 0.20); again, this behavior can be described using adsorption isotherms for Na^+; the fastest rates in this pH range are slightly slower than the rates in the near-neutral pH range because alkaline pH values require a finite amount of Na^+ from NaOH.

The data used in calculation of magnesite rate parameters are for low ionic strength only (≤0.1) in the acidic pH range of 3 to 5, and in the circum-neutral pH range of 5-8 all data are used; these data are denoted with open triangles in Figure 2. For non-linear regression, these data are simultaneously fit to a form of eqn. (9) from which the term for the basic mechanism has been omitted; the data were obtained from experiments at 25 °C only, so the activation energy is omitted as well

$$\frac{dm}{dt} = -(K_{acid}^{298.15K} a_{H^+}^{n_1} + K_{neutral}^{298.15K}) \qquad (13)$$

For linear regression, the data are fit to a modified form of eqn. (11) for the acidic mechanism

$$\log(rate) = \log K_{acid}^{298.15K} - n_{H^+} pH \qquad (14)$$

and for the neutral mechanism, a simple average is calculated, yielding the rate constants at 25 °C and an acidic mechanism (positive) reaction order. The gray curves in Figure 2 show the results of the non-linear regression, the black dashed straight lines in Figure 2 show separately the results for both the acidic and neutral mechanisms, and the black curve represents their sum.

Since data are lacking for the temperature dependence of magnesite dissolution rates, the activation energies for calcite (discussed below) are used as a first approximation, allowing for the calculation of the pre-exponential factors. The chemical affinity factors p and q are taken directly from Pokrovsky and Schott (1999), and were derived from experiments in which the initial solutions contained varying amounts of Mg^{2+} and CO_3^{2-}. Data for the rate parameters derived from the regression are summarized in Table 2.

Neither piecewise linear regression nor non-linear curve fitting provide a good fit to the data under acidic and basic pH conditions, because of the inability of the selected rate equations to account for surface adsorption of various rate catalyzing and inhibiting species. However, the non-linear curve fitting method allows the calculation of rate parameters that are accurate to a first approximation over a wide range of circum-neutral pH.
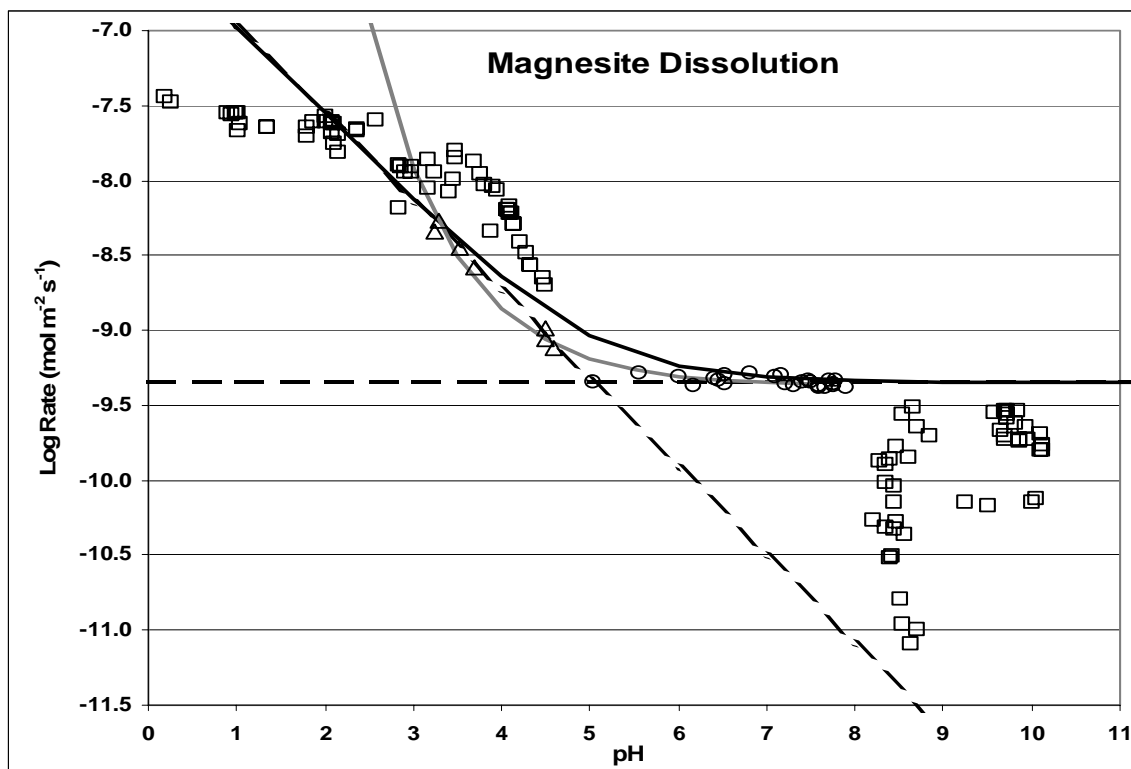
Figure 2. Rates of magnesite dissolution at 25 °C and pH from 0.19 to 10.13. Data 25 °C from Pokrovsky and Schott, 1999; open triangles, data used in piecewise linear regression; open squares, other data. Dashed lines, results from piecewise linear regression of acidic and neutral mechanisms. Black curves, sum of results from piecewise linear regression. Gray curve, results from non-linear curve fitting.

Table 2. Dissolution Rate Parameters.

	Acid Mechanism				Neutral Mechanism		
	[a]A	[b]log k	[c]E	[d]n	[a]A	[b]log k	[c]E
Linear Regression	1.40E-04	-6.38	14.5	0.589	6.05E-06	-9.34	23.5
Non-Linear Regression	1.62E+32	32.21	14.5	0.448	4.27E-10	-9.37	23.5
	p	*q*			*p*	*q*	
[e]Chemical Affinity	4.00	1.00			--	--	

a. Arrhenius pre-exponential factor A, mole m^{-2} s^{-1} for use with equation (5).
b. Log rate constant k computed from A and E, 25°C, pH=0, log mole m^{-2} s^{-1} for use with equation (6).
c. Arrhenius activation energy E, kJ $mole^{-1}$.
d. Reaction order n with respect to H^{+}.
e. Chemical affinity parameters *p* and *q* default to unity if not specified.

2.3 Limitations and Uncertainties

Application of kinetics to geochemical modeling is subject to a number of limitations resulting from uncertainties in the experimental methods and materials from which the rate parameters are derived, and from the modeling software used for the simulations. Ideally, experimental data would be available over wide ranges of temperature and pressure for dissolution of perfectly crystalline minerals under conditions far from equilibrium i.e. where the chemical affinity is large, so that further increases in chemical affinity lead to no observed increase in reaction rates. Additional data would be available to quantify slowing of reaction rates as the chemical affinity decreases, as equilibrium is approached with increasing concentration of dissolved components that are contained in the mineral structure. Further data would be available for dissolved components not contained in the mineral structure that might catalyze or inhibit the reactions. Further, data would also be available to account for varying mineral compositions in each solid solutions series. Finally, data would be available for minerals that are not perfectly crystalline, i.e. minerals with crystal defects, cation disordering, or igneous exsolution features — for which the required number of experiments would be nearly infinite. Most of these data do not yet exist, and for those minerals for which data exist, data are available mostly for experiments conducted only under conditions that are far from equilibrium, and values for p and q are assumed to be equal to unity, which is likely incorrect.

Additional limitations include various factors of experimental design and solid phase preparation: 1) stirring rates may be insufficient to ensure that there are not concentration gradients near mineral surfaces, which may slow dissolution reactions(Alkattan et al., 1998; Metz and Ganor, 2001), especially for minerals that have fast overall rates such as calcite (Alkattan et al., 1998); 2) in some experimental reactor designs, particle abrasion may lead to faster apparent rates; 3) grinding of samples may produce surface fines which can be removed with solvents, but also may produce particles which may chemically re-bind to mineral surfaces (Petrovich, 1981b), and/or produce crystal defects at or near mineral surfaces (Bloom, 1983; Furrer et al., 1993; Nagy, 1995; Nagy et al., 1991; Petrovich, 1981b; Wieland and Stumm, 1992), which may lead to faster initial apparent rates; and 4) there is also a degree of uncertainty as to whether the reactive surface area can be equated with the geometric or BET surface areas (Aagaard and Helgeson, 1982; Gautier et al., 2001; Helgeson et al., 1984; Lasaga, 1998). At least one study (Gautier et al., 2001) of quartz dissolution has shown that an increase in BET surface area during dissolution consists primarily of un-reactive etch pit walls, and concludes that geometric surface area provides for more accurate calculation of dissolution rates.

The rate equation we have selected, eqn. (7), is also subject to further limitations. It does not account for temperature dependence of the pre-exponential factor resulting from variation in the velocity in solution of dissolved species, nor does it does not account for apparent pH dependence of the activation energy, which can be described using adsorption isotherms (Lasaga, 1995). The selected equation applies only to bulk dissolution rates, and does not account for crystallographic control of mineral dissolution, i.e. variation of dissolution rates on different crystallographic surface planes.

3. RESULTS

3.1 Tectosilicates

3.1.1 SiO$_2$ Polymorphs

3.1.1.1 Quartz

Rate data and parameters for quartz from several sources were evaluated (Bennett, 1991; Bennett et al., 1988; Bird et al., 1986; Blake and Walter, 1999; Brady, 1992; Dove, 1994; Dove, 1999; Dove and Crerar, 1990; Dove and Elston, 1992; Dove and Nix, 1997; Gautier et al., 2001; Knauss and Copenhaver, 1995; Knauss and Wolery, 1988; Rimstidt and Barnes, 1980; Schwartzentruber et al., 1987; Tester et al., 1994; Welch and Ullman, 1992). Data from Tester et al. were selected for the neutral pH mechanism because the authors were able to correlate consistently their experimental results with the results of many workers, including Bennett (1991), Berger et al. (1994), Blum et al. (1990), Brady and Walther (1990), Dove and Crerar (1990), Kitahara (1960), Rimstidt and Barnes (1980), Siebert et al. (1963), Van Lier et al. (1960), and Weill and Fyfe (1964) at temperatures from 25 to 625 °C. In the acidic region, dissolution rates are apparently independent of pH (Dove, 1994; Knauss and Wolery, 1988; Rimstidt and Barnes, 1980), and can be equated with rates in the neutral region at identical T and P. The data used to regress rate parameters using eqn. (11) for neutral pH are shown in Table 3.

Table 3. Quartz dissolution Rate Data in Pure H$_2$O.

T, °C	T, K	[a]log k	[b]log k	T, °C	T, K	[a]log k	[b]log k
23	296.15	-13.41	-14.24	400	673.15	-4.45	--
23	296.15	-13.38	-14.21	400	673.15	-4.35	--
50	323.15	-12.22	-13.05	440	713.15	-4.16	--
50	323.15	-12.21	-13.04	440	713.15	-4.35	--
50	323.15	-12.19	-13.02	440	713.15	-4.51	--
70	343.15	-11.33	-12.18	480	753.15	-4.41	--
100	373.15	-10.19	-11.03	480	753.15	-4.19	--
100	373.15	-10.22	-11.06	70	343.15	-12.16	-12.22
100	373.15	-10.20	-11.04	80	353.15	-11.46	-11.52
100	373.15	-10.45	-11.3	90	363.15	-11.16	-11.22
125	398.15	-9.32	-10.17	248	521.15	-6.08	--
125	398.15	-9.20	-10.05	250	523.15	-5.98	--
125	398.15	-9.08	-9.93	269	542.15	-5.84	--
125	398.15	-9.17	-10.02	291	564.15	-5.55	--
125	398.15	-9.19	-10.03	315	588.15	-5.22	--
125	398.15	-9.55	-10.4	332	605.15	-5.02	--
125	398.15	-9.75	-10.6	400	673.15	-3.95	--
125	398.15	-9.58	-10.43	625	898.15	-2.97	--
125	398.15	-9.82	-10.67	105	378.15	-10.27	-11.5
125	398.15	-9.59	-10.44	145	418.15	-8.36	-9.59
150	423.15	-8.42	-9.26	170	443.15	-8.43	-9.66
150	423.15	-8.48	-9.33	265	538.15	-6.56	-7.79

Table 3. Quartz dissolution Rate Data in Pure H$_2$O - continued.

T, °C	T, K	[a]log k	[b]log k	T, °C	T, K	[a]log k	[b]log k
175	448.15	-8.38	-9.23	305	578.15	-6.14	-7.37
175	448.15	-8.34	-9.19	80	353.15	-10.75	-11.18
175	448.15	-8.38	-9.23	80	353.15	-10.89	-11.25
175	448.15	-8.28	-9.12	80	353.15	-10.99	-11.52
175	448.15	-8.32	-9.16	200	473.15	-7.63	-7.93
200	473.15	-7.88	-8.72	200	473.15	-7.35	-7.65
200	473.15	-7.82	-8.67	200	473.15	-7.28	-7.58
200	473.15	-7.05	--	200	473.15	-7.38	-7.68
200	473.15	-7.21	--	200	473.15	-7.26	-7.56
200	473.15	-7.30	--	201	474.15	-7.43	-7.73
250	523.15	-6.67	--	250	523.15	-6.74	-7.04
184	457.15	-7.96	--	300	573.15	-5.97	-6.27
184	457.15	-8.10	--	300	573.15	-6.01	-6.31
184.5	457.65	-8.32	--	300	573.15	-6.15	-6.45
202	475.15	-7.31	--	40	313.15	-13.13	-12.7
202.5	475.65	-7.49	--	50	323.15	-11.73	-12.3
203	476.15	-7.29	--	60	333.15	-11.33	-11.9
215	488.15	-7.05	--	70	343.15	-10.83	-11.4
221	494.15	-6.89	--	70	343.15	-10.93	-11.5
221	494.15	-6.96	--	200	473.15	-6.84	-7.92
221	494.15	-7.12	--	300	573.15	-5.38	-6.46
253	526.15	-6.38	--	300	573.15	-5.63	-6.71
255	528.15	-6.50	--				

a. Log mole m^{-2} s^{-1}, calculated by Tester et al. (1994) using geometric surface area
b. Log mole m^{-2} s^{-1}, calculated by Tester et al. (1994) using BET surface area

Another series of studies from Dove and co-workers (Dove, 1994; Dove, 1999; Dove and Crerar, 1990; Dove and Elston, 1992; Dove and Nix, 1997) demonstrate an important phenomenon, that sodium ion catalyzes the OH^--catalyzed (base) dissolution reaction mechanism (as do Li, K, Mg, Ca, and Ba). These data were not used because adsorption isotherms must be used to implement their results; therefore, we use the results from Knauss and Wolery (1988) directly for rates under alkaline conditions, which are given terms of reaction order with respect to OH^-.

Results from the regression calculations for the neutral mechanism using both geometric and BET surface area performed herein and those performed by Tester et al. (1994), and results from Knauss and Wolery (1988) for the base mechanism are summarized in Table 4. The source of the small difference between our results and those of Tester et al. (1994) is uncertain. The chemical affinity parameters were not determined, and the chemical affinity parameters p and q are assumed to be unity.

Table 4. Quartz Dissolution Rate Parameters.

	Linear Regression Parameters							
	Neutral Mechanism				Base Mechanism			
	[a]A	[b]log k	[c]E		[a]A	[b]log k	[c]E	[d]n
[e]quartz	333	-13.40	90.9		--	--	--	--
[f]quartz	276	-13.34	90.1		--	--	--	--
[g]quartz	23.3	-13.99	87.6		--	--	--	--
[h]quartz	24	-13.99	87.7		--	--	--	--
[i]quartz	--	--	--		10	-16.29	108366	-0.5

a. Arrhenius pre-exponential factor A, mole m^{-2} s^{-1} for use with equation (5).
b. log rate constant k computed from A and E, 25°C, pH=0, log mole m^{-2} s^{-1} for use with equation (6).
c. Arrhenius activation energy E, kJ $mole^{-1}$.
d. Reaction order n with respect to H^+.
e. Calculated using geometric surface area.
f. Calculated by Tester et al. (1994)using geometric surface area.
g. Calculated using BET surface area.
h. Calculated by Tester et al. (1994)using BET surface area.
i. From Knauss and Wolery (1988), A adjusted here from 491 to 10 to be consistent with the results of Tester et al. (1994).

3.1.1.2 Amorphous SiO_2, Cristobalite, and SiO_2 Polymorph Precipitation

Rate data and calculated rate equation parameters for amorphous silica dissolution from Icenhower and Dove (2000), and Rimstidt and Barnes (1980) were evaluated. Data from Icenhower and Dove (2000) were selected because they conducted many individual experimental runs, and they were able to correlate their data with data from other workers. The rate parameters are summarized in Table 6. The presence of small amounts of NaCl in solution significantly enhances dissolution rates (21x at 0.05m Incenhower and Dove, 2000), this can be accounted for by using adsorption isotherms, but cannot be described with our selected rate equations (eqns. 5 and 6)

Rate parameters for α-cristobalite and β-cristobalite are compiled directly from Rimstidt and Barnes (1980). The rate parameters were calculated by the authors under the assumption that the precipitation rates for all of the SiO_2 polymorphs are equal (Rimstidt and Barnes, 1980), and eqn. (8). These data are also summarized in Table 6.

Table 5. Amorphous Silica Dissolution Rate Data in Pure H_2O.

T, °C	T, K	[a]log k	T, °C	T, K	[a]log k
40	313.15	-11.36	80	353.15	-10.47
40	313.15	-11.17	80	353.15	-10.47
60	333.15	-10.75	250	523.15	-6.59
60	333.15	-10.84	225	498.15	-6.86
60	333.15	-10.63	225	498.15	-6.96
60	333.15	-10.57	200	473.15	-7.4
60	333.15	-10.65	200	473.15	-7.34
60	333.15	-10.99	175	448.15	-7.89
60	333.15	-10.97	175	448.15	-7.74

Table 5. Amorphous Silica Dissolution Rate Data in Pure H_2O - continued.

T, °C	T, K	[a]log k	T, °C	T, K	[a]log k
60	333.15	-10.92	150	423.15	-8.41
60	333.15	-10.98	150	423.15	-8.53
60	333.15	-10.93	225	498.15	-6.86
60	333.15	-10.97	225	498.15	-7.05
60	333.15	-10.93	200	473.15	-7.24
60	333.15	-11.05	200	473.15	-7.27
60	333.15	-11.22	175	448.15	-7.97
60	333.15	-11.2	175	448.15	-8.1
60	333.15	-11.15	150	423.15	-8.24
60	333.15	-11.18	125	398.15	-8.75
60	333.15	-11.09	100	373.15	-9.36
80	353.15	-10.28	100	373.15	-9.54

a. Log mole m^{-2} s^{-1} for use with equation (6); data for experiments in de-ionized water only, from Icenhower and Dove, 2000.

Table 6. Amorphous Silica and Cristobalite Dissolution, and Silica Polymorph Precipitation Rate Parameters.

	Neutral Mechanism		
Dissolution	[a]**A**	[b]**log k**	[c]**E**
[d]Amorphous Silica	6.65E+00	-12.23	74.5
[e]Amorphous Silica	1.01E+01	-12.31	76.0
[f]Amorphous Silica	1.85E-01	-12.77	68.7
[f]α-cristobalite	1.20E-01	-12.31	65.0
[f]β-cristobalite	7.60E-02	-12.14	62.9
Precipitation			
[f]All SiO_2 polymorphs	2.02E-01	-9.42	49.8

a. Arrhenius pre-exponential factor A, mole m^{-2} s^{-1} for use with equation (5).
b. log rate constant k at 25°C and pH = 0, log mole m^{-2} s^{-1} for use with equation (6).
c. Arrhenius activation energy E, kJ $mole^{-1}$.
d. Reported values for k and E from Incenhower and Dove (2000), A calculated herein.
e. A and E regressed using data from Incenhower and Dove (2000), Table 5; k calculated from A and E herein.
f. Reported values for k and E from Rimstidt and Barnes (1980); A calculated from k.

3.1.2 Feldspars

3.1.2.1 Plagioclase Feldspars

Plagioclase dissolution rate data were evaluated from Alekseyev et al. (1997), Amrhein and Suarez (1988), Amrhein and Suarez (1992), Berg and Banwart (2000), Bevan and Savage (1989), Blake and Walter (1996), Blake and Walter (1999), Blum and Stillings (1995), Brady and Walther (1989), Brantley and Stillings (1994), Burch et al. (1993), Busenberg and Clemency (1976), Carroll and Knauss (2001), Casey et al. (1991), Casey and Sposito (1992), Chen and Brantley (1997), Chen et al. (2000), Chou and Wollast (1984), Chou and Wollast (1985), Fenter et al. (2003), Fleer and Johnston (1986),Gautier et al. (1994), Hajash et al. (1998), Helgeson et al. (1984) Holdren and Berner (1979), Holdren and Speyer (1987), Hellman (1994b), Hellman (1994a), Hellman (1995), Knauss and Wolery (1986), Knauss and Copenhaver (1995), Lagache (1965), Lagache (1976), Lüttge et al. (1999), Manley and Evans (1986), Murakami et al. (1998), Murphy and Helgeson (1987; 1989), Oelkers et al. (1994), Oelkers and Schott (1995), Oelkers and Gislason (2001), Oelkers (2001b), Oxburgh et al. (1994), Rafal'skiy et al. (1990), Rafal'skiy and Prisyagina (1991), Stillings et al. (1995), Stillings et al. (1996), Swoboda-Colberg and Drever (1993), Talman and Nesbitt (1988), Taylor et al. (2000a), Tsuzuki and Suzuki (1980), Teng et al. (2001), Utsunomiya et al. (1999), Welch and Ullman (1992), Welch and Ullman (1993), Welch and Ullman (1996), and Welch and Ullman (2000).

Unlike the plagioclase endmember albite discussed above, dissolution rates for the remainder of the plagioclase solid solution series are not as well constrained. Most of the available data are biased toward low temperature and near-neutral to acidic pH (Blum and Stillings, 1995). One important but poorly quantified observation is that dissolution rates increase continuously with increasing anorthite content. This effect is more pronounced for more anorthitic compositions; at 25°C and pH = 5, rates increase by approximately one order of magnitude from albite (log k ≈ -12 log mol m^{-2} s^{-1}) to labradorite (log k ≈ -11 log mol m^{-2} s^{-1}), and by almost three orders of magnitude between labradorite and anorthite (log k ≈ -8 log mol m^{-2} s^{-1}) (Blum and Stillings, 1995). This effect diminishes with decreasing pH, and the difference in the logarithm of rate approaches a linear relation with respect to composition at pH = 2. A second observation that has not been well quantified is that dissolution activation energy decreases with increasing anorthite content.

Our general strategy is to identify data from various workers that are consistent with one another as primary constraints, and to interpolate pre-exponential factors and activation energies that are consistent with the data. Wherever possible rate data are selected from experiments in flow-through reactors, where dissolution rates were measured using the concentration of dissolved silica in the reactor output fluid, and where silica concentrations were allowed to reach steady-state, thus indicating steady-state thickness of any possible leached layer. One issue not addressed in the cited works is the extent to which cation disorder in the minerals may affect the given rates. Data were selected for the plagioclase solid solution series, and are summarized in tables as follows: albite, Table 7; oligoclase, Table 8; andesine, Table 9; labradorite, Table 10; bytownite, Table 11; anorthite, Table 12. Primary constraints are the data and results for albite (T = 25 to 300 °C, pH = 1.3 to 10.3) and anorthite (T = 8 to 95 °C, pH = 2.43 to 10.2), with interpolation obtained graphically for the components of the solid solution. The derived parameters are summarized in Table 13. Chemical affinity parameters p and q for albite are

0.760 and 90.0 respectively (Alekseyev et al., 1997), but their use in modeling should be limited to conditions near the experimental conditions under which they were obtained, 300 °C and pH = 9.

Table 7. Albite Dissolution Rate Data.

Acid Mechanism			Neutral Mechanism			Base Mechanism		
T, °C	pH	[a]log k	T, °C	pH	log k	T, °C	pH	[a]log k
25	1.1	-10.25	25	5.1	-11.82	25	9.95	-10.97
25	2.05	-10.55	25	5.35	-11.75	25	9.95	-11.05
25	2.45	-10.82	25	5.47	-11.65	25	9.95	-11.13
25	2.9	-11.25	25	5.63	-11.83	25	10.6	-10.95
25	3	-11.1	25	5.63	-11.92	25	11.2	-10.55
25	3.5	-11.4	25	5.73	-11.92	25	11.55	-10.6
25	4.1	-11.47	25	7.73	-11.83	25	12.3	-10.38
100	2.0	-9.05	25	7.95	-11.67	100	10.3	-8.92
100	2.0	-9.07	100	5.7	-9.47	200	9.3	-7.15
100	4.0	-9.00	100	5.7	-9.62	300	8.6	-6.25
100	4.0	-9.50	100	7.7	-9.35	300	8.6	-6.01
100	4.0	-9.38	100	8.2	-9.77	300	9.2	-5.97
200	2.0	-6.72	172	5.7	-8.09	300	9.2	-5.46
200	2.0	-6.63	191	5.6	-7.61	300	10.0	-5.29
200	2.0	-6.80	200	5.6	-7.79			
200	4.0	-7.54	200	7.5	-7.79			
300	1.3	-5.13	222	5.6	-7.27			
300	2.2	-5.17	300	5.7	-6.35			
300	2.2	-5.57	300	5.7	-6.44			
300	3.4	-6.06	300	5.7	-6.30			
300	4.0	-6.36	300	6.8	-6.13			
			300	7.4	-6.30			
			300	7.7	-5.92			
			300	7.7	-6.03			

a. Log mole m^{-2} s^{-1}. Data at 25 °C from Chou and Wollast (1985), for Amelia albite, composition not specified. Data from 100 to 300 °C from Hellman (1984), for Amelia Albite, $Ab_{100}An_0Or_0$ (1984).

Table 8. Oligoclase Dissolution Rate Data.

an	ab	or	T, °C	[b]pH	[c]log k	Source
20	--	--	25	2	-10.85	Casey et al., 1991
20	--	--	25	2	-10.44	Casey et al., 1991
21	--	--	25	2	-10.69	Casey et al., 1991
13	--	--	25	3	-11.47	Oxburgh et al., 1994
20	--	--	25	3	-10.94	Holdren and Speyer, 1987
13	--	--	25	3.6	-11.70	Oxburgh et al., 1994
13	--	--	25	4	-11.92	Oxburgh et al., 1994
13	--	--	25	4.6	-12.22	Oxburgh et al., 1994
13	--	--	25	5.1	-12.10	Oxburgh et al., 1994
24	70	6	25	5.3	-11.59	Busenberg and Clemency, 1976
22	73	5	25	5.4	-11.63	Stillings et al., 1996
13	--	--	25	7	-11.96	Oxburgh et al., 1994

a. -- = Not given.
b. Acid mechanism, pH 2-4.6; neutral mechanism, pH 5.1-7.
c. Log mole m^{-2} s^{-1}.

Table 9. Andesine Dissolution Rate Data.

[a]Composition						
an	ab	or	T, °C	[b]pH	[c]log k	Source
46	--	--	25	2	-10.16	Casey et al., 1991
46	--	--	25	2	-10.01	Casey et al., 1991
46	--	--	25	3	-10.64	Holdren and Speyer, 1987
49	--	--	22	3.1	-9.78	Welch & Ullman., 1993
49	--	--	22	3.1	-9.27	Welch & Ullman., 1993
46	--	--	25	3.1	-10.65	Oxburgh et al., 1994
47	51	2	25	3.13	-10.62	Stillings et al., 1996
49	--	--	22	3.8	-10.12	Welch & Ullman., 1993
49	--	--	22	4.1	-9.81	Welch & Ullman., 1993
46	--	--	25	4.1	-11.15	Oxburgh et al., 1994
47	51	2	25	4.11	-11.15	Stillings et al., 1996
47	51	2	25	5.08	-11.24	Stillings et al., 1996
46	--	--	25	5.1	-11.24	Oxburgh et al., 1994
49	--	--	22	5.3	-10.47	Welch & Ullman., 1993
43	50	8	25	5.3	-11.86	Busenberg and Clemency, 1976
49	--	--	22	5.6	-10.51	Welch & Ullman., 1993
43	50	7	25	5.61	-11.52	Stillings et al., 1996
49	--	--	22	5.7	-10.78	Welch & Ullman., 1993
49	--	--	22	5.8	-10.74	Welch & Ullman., 1993
35	65	0	250	6.83	-8.48	Rafal'skiy and Prisyagina, 1991
47	51	2	25	7.22	-11.21	Stillings et al., 1996
46	--	--	25	7.3	-11.29	Oxburgh et al 1994
35	65	0	150	7.46	-9.39	Rafal'skiy and Prisyagina, 1991
49	--	--	22	7.7	-10.7	Welch & Ullman., 1993
49	--	--	22	9	-10.31	Welch & Ullman., 1993

a. -- = Not given.
b. Acid mechanism, pH 2-4.11; Neutral mechanism, pH 5.1-7.7; base mechanism, pH 9.
c. Log mole m^{-2} s^{-1}.

Table 10. Labradorite Dissolution Rate Data.

[a]Composition			T, °C	[b]pH	[c]log k	Source
an	ab	or				
51	--	--	230	0.41	-6.44	Tsuzuki and Suzuki, 1980
51	--	--	245	0.45	-6.48	Tsuzuki and Suzuki, 1980
51	--	--	230	0.81	-6.35	Tsuzuki and Suzuki, 1980
51	--	--	245	0.84	-6.71	Tsuzuki and Suzuki, 1980
51	--	--	230	0.96	-6.71	Tsuzuki and Suzuki, 1980
51	--	--	245	0.98	-6.71	Tsuzuki and Suzuki, 1980
51	--	--	230	1.21	-7.6	Tsuzuki and Suzuki, 1980
51	--	--	245	1.23	-7.48	Tsuzuki and Suzuki, 1980
51	--	--	230	1.67	-7.48	Tsuzuki and Suzuki, 1980
51	--	--	245	1.69	-7.44	Tsuzuki and Suzuki, 1980
60	--	--	25	2	-9.85	Busenberg and Clemency, 1976
61	--	--	25	3.2	-10.6	Casey et al., 1991
61	--	--	25	3.2	-10.5	Taylor et al., 2000
61	--	--	25	3.2	-10.5	Taylor et al., 2000
61	--	--	25	3.2	-10.6	Taylor et al., 2000
61	--	--	25	3.2	-10.5	Taylor et al., 2000
61	--	--	25	3.2	-10.6	Taylor et al., 2000
60	--	--	31	3.2	-9.45	Carroll and Knauss, 2001
60	--	--	60	3.2	-9.02	Carroll and Knauss, 2001
60	--	--	61	3.2	-8.37	Carroll and Knauss, 2001
60	--	--	100	3.2	-8.34	Carroll and Knauss, 2001
60	--	--	30	3.21	-9.53	Carroll and Knauss, 2001
60	--	--	130	3.22	-7.67	Carroll and Knauss, 2001
60	--	--	100	3.24	-8.11	Carroll and Knauss, 2001
60	--	--	130	3.24	-7.66	Carroll and Knauss, 2001
60	--	--	100	3.25	-8.09	Carroll and Knauss, 2001
60	--	--	60	3.29	-8.83	Carroll and Knauss, 2001
60	--	--	100	3.29	-8.31	Carroll and Knauss, 2001
60	--	--	130	3.3	-7.72	Carroll and Knauss, 2001
60	--	--	100	3.37	-8.52	Carroll and Knauss, 2001
60	--	--	150	3.5	-7.18	Carroll and Knauss, 2001
57	43	0	200	4.88	-8.48	Lagache, 1965
53	44	3	25	5.3	-11.9	Taylor et al., 2000
70	--	--	80	6	-9.01	Blake and Walter, 1999

a. -- = Not given.
b. Acid mechanism, pH 0.84-6.
c. Log mole m^{-2} s^{-1}.

Table 11. Bytownite Dissolution Rate Data.

[a]Composition			T, °C	pH	[b]log k	Source
an	ab	or				
76	--	--	25	2	-9.74	Oxburgh et al., 1994
76	--	--	25	3	-9.7	Oxburgh et al., 1994
76	--	--	25	3.1	-10.31	Oxburgh et al., 1994
77	--	--	35	3.2	-11.13	Welch and Ullman, 2000
76	--	--	25	3.8	-10.91	Oxburgh et al., 1994
77	--	--	22	4	-8.69	Welch and Ullman, 1993
76	--	--	25	4.4	-10.91	Oxburgh et al., 1994
76	--	--	25	4.75	-8.67	Casey et al., 1991
77	--	--	22	4.9	-8.89	Welch and Ullman, 1993
76	--	--	25	5	-10.97	Oxburgh et al., 1994
76	--	--	25	5.3	-9.91	Holdren and Speyer, 1987
77	--	--	5	5.65	-11.86	Welch and Ullman, 2000
77	--	--	20	5.65	-11.4	Welch and Ullman, 2000
76	24	0	25	5.65	-10.76	Stillings et al., 1996
77	22	--	25	5.65	-11.97	Busenberg and Clemency, 1976
77	--	--	22	5.7	-10.2	Welch and Ullman, 1993
77	--	--	22	7.2	-10.12	Welch and Ullman, 1993

a. -- = Not given.
b. Acid mechanism, pH 2-5.3; Neutral mechanism, pH 5.65-7.2.
c. Log mole m^{-2} s^{-1}.

Table 12. Anorthite Dissolution Rate Data.

[a]Composition			T, °C	pH	[b]log k	Source
an	ab	or				
100	0	0	25	2	-10.32	Fleer, 1982
100	0	0	50	2	-9.72	Fleer, 1982
100	0	0	70	2	-9.59	Fleer, 1982
92	--	--	25	3	-9.77	Holdren and Speyer, 1987
93	--	--	25	3.6	-10.24	Amrhein and Suarez, 1992
unk	--	--	25	4	-10.65	Bailey, 1974
unk	--	--	45	4	-10.35	Bailey, 1974
unk	--	--	65	4	-10.35	Bailey, 1974
93	--	--	25	4.45	-10.83	Amrhein and Suarez, 1992
93	--	--	25	4.65	-11.33	Amrhein and Suarez, 1992
93	--	--	25	4.7	-11.27	Amrhein and Suarez, 1992
93	--	--	25	6	-10.14	Amrhein and Suarez, 1992
93	--	--	25	6	-10.69	Amrhein and Suarez, 1992
100	0	0	25	6.7	-10.83	Berg and Banwart, 2000
100	0	0	25	7.4	-11.15	Berg and Banwart, 2000
93	--	--	25	7.65	-11.37	Amrhein and Suarez, 1992
100	0	0	25	8.1	-11.11	Berg and Banwart, 2000
100	0	0	25	8.4	-10.82	Berg and Banwart, 2000
100	0	0	70	10.2	-11.41	Fleer, 1982
97	--	--	45	2.46	-6.79	Oelkers and Schott, 1995
97	--	--	45	2.47	-6.86	Oelkers and Schott, 1995
97	--	--	45	2.65	-7.09	Oelkers and Schott, 1995
97	--	--	45	2.56	-7.01	Oelkers and Schott, 1995
97	--	--	45	2.56	-7.06	Oelkers and Schott, 1995
97	--	--	45	2.58	-6.97	Oelkers and Schott, 1995
97	--	--	45	2.48	-6.94	Oelkers and Schott, 1995
97	--	--	60	2.53	-6.65	Oelkers and Schott, 1995
97	--	--	60	2.78	-7.09	Oelkers and Schott, 1995
97	--	--	60	2.54	-6.75	Oelkers and Schott, 1995
97	--	--	60	2.65	-6.94	Oelkers and Schott, 1995
97	--	--	60	2.56	-6.82	Oelkers and Schott, 1995
97	--	--	60	2.52	-6.76	Oelkers and Schott, 1995
97	ab	--	60	2.52	-6.74	Oelkers and Schott, 1995
97	--	--	60	2.51	-6.58	Oelkers and Schott, 1995
97	--	--	60	2.72	-6.92	Oelkers and Schott, 1995
97	--	--	60	2.54	-6.77	Oelkers and Schott, 1995
97	--	--	60	2.77	-7.04	Oelkers and Schott, 1995
97	--	--	60	2.52	-6.70	Oelkers and Schott, 1995
97	--	--	60	2.62	-6.87	Oelkers and Schott, 1995
97	--	--	60	2.50	-6.68	Oelkers and Schott, 1995
97	--	--	60	2.65	-6.96	Oelkers and Schott, 1995
97	--	--	60	2.78	-7.16	Oelkers and Schott, 1995
97	--	--	60	2.53	-6.78	Oelkers and Schott, 1995

Table 12. Anorthite Dissolution Rate Data - continued.

an	ab	or	T, °C	pH	log k	Source
97	--	--	60	2.74	-7.13	Oelkers and Schott, 1995
97	--	--	60	2.68	-7.00	Oelkers and Schott, 1995
97	--	--	60	2.63	-6.94	Oelkers and Schott, 1995
97	--	--	60	2.81	-7.21	Oelkers and Schott, 1995
97	--	--	60	2.59	-6.93	Oelkers and Schott, 1995
97	--	--	60	2.56	-6.89	Oelkers and Schott, 1995
97	--	--	60	2.71	-7.14	Oelkers and Schott, 1995
97	--	--	60	2.54	-6.90	Oelkers and Schott, 1995
97	--	--	60	2.56	-6.64	Oelkers and Schott, 1995
97	--	--	60	2.60	-6.77	Oelkers and Schott, 1995
97	--	--	60	2.75	-7.06	Oelkers and Schott, 1995
97	--	--	60	2.66	-6.92	Oelkers and Schott, 1995
97	--	--	60	2.51	-6.70	Oelkers and Schott, 1995
97	--	--	60	2.55	-6.85	Oelkers and Schott, 1995
97	--	--	60	2.70	-7.13	Oelkers and Schott, 1995
97	--	--	60	2.61	-7.02	Oelkers and Schott, 1995
97	--	--	60	2.72	-6.96	Oelkers and Schott, 1995
97	--	--	60	2.58	-6.72	Oelkers and Schott, 1995
97	--	--	60	2.77	-7.10	Oelkers and Schott, 1995
97	--	--	60	2.65	-6.89	Oelkers and Schott, 1995
97	--	--	60	2.63	-6.85	Oelkers and Schott, 1995
97	--	--	60	2.46	-6.70	Oelkers and Schott, 1995
97	--	--	60	2.41	-6.55	Oelkers and Schott, 1995
97	--	--	60	2.62	-6.81	Oelkers and Schott, 1995
97	--	--	60	2.51	-6.61	Oelkers and Schott, 1995
97	--	--	60	2.55	-6.72	Oelkers and Schott, 1995
97	--	--	60	2.61	-6.88	Oelkers and Schott, 1995
97	--	--	60	2.53	-6.74	Oelkers and Schott, 1995
97	--	--	60	2.58	-6.94	Oelkers and Schott, 1995
97	--	--	60	2.67	-6.77	Oelkers and Schott, 1995
97	--	--	60	3.08	-7.52	Oelkers and Schott, 1995
97	--	--	60	2.90	-7.22	Oelkers and Schott, 1995
97	--	--	60	2.87	-7.16	Oelkers and Schott, 1995
97	--	--	60	3.00	-7.40	Oelkers and Schott, 1995
97	--	--	60	2.91	-7.28	Oelkers and Schott, 1995
97	--	--	60	2.94	-7.38	Oelkers and Schott, 1995
97	--	--	75	2.52	-6.53	Oelkers and Schott, 1995
97	--	--	75	2.54	-6.63	Oelkers and Schott, 1995
97	--	--	75	2.71	-6.94	Oelkers and Schott, 1995
97	--	--	75	2.56	-6.69	Oelkers and Schott, 1995
97	--	--	75	2.61	-6.78	Oelkers and Schott, 1995
97	--	--	75	2.67	-6.86	Oelkers and Schott, 1995

Note: The Composition column spans an, ab, or. The log k column is footnoted [b], Composition is footnoted [a].

Table 12. Anorthite Dissolution Rate Data - continued.

[a]Composition						
an	ab	or	T, °C	pH	[b]log k	Source
97	--	--	75	2.51	-6.63	Oelkers and Schott, 1995
97	--	--	75	2.50	-6.61	Oelkers and Schott, 1995
97	--	--	95	2.65	-6.71	Oelkers and Schott, 1995
97	--	--	95	2.60	-6.61	Oelkers and Schott, 1995
97	--	--	95	2.53	-6.48	Oelkers and Schott, 1995
97	--	--	95	2.73	-6.91	Oelkers and Schott, 1995
97	--	--	95	2.58	-6.59	Oelkers and Schott, 1995
97	--	--	95	2.55	-6.54	Oelkers and Schott, 1995
97	--	--	95	2.68	-6.80	Oelkers and Schott, 1995
97	--	--	95	2.58	-6.64	Oelkers and Schott, 1995

Table 13. Plagioclase Dissolution Rate Parameters.

	Acid Mechanism			Neutral Mechanism		Base Mechanism		
	[a]log k	[b]E	[c]n	[a]log k	[b]E	[a]log k	[b]E	[c]n
Albite	-10.16	65.0	0.457	-12.56	69.8	-15.60	71.0	-0.572
Oligoclase	-9.67	65.0	0.457	-11.84	69.8	--	--	--
Andesine	-8.88	53.5	0.541	-11.47	57.4	--	--	--
Labradorite	-7.87	42.1	0.626	-10.91	45.2	--	--	--
Bytownite	-5.85	29.3	1.018	-9.82	31.5	--	--	--
Anorthite	-3.50	16.6	1.411	-9.12	17.8	--	--	--

a. Rate constant k computed from A and E, 25°C, pH = 0, mole m^{-2} s^{-1}
b. Arrhenius activation energy E, kJ $mole^{-1}$.
c. Reaction order n with respect to H^+

3.1.2.2 K-feldspar

Dissolution rate data were evaluated from Alekseyev et al. (1997), Bevan and Savage (1989), Blake and Walter (1996), Blake and Walter (1999), Blum and Stillings (1995), Busenberg and Clemency (1976), Fenter et al. (2003), Gautier et al. (1994), Helgeson et al. (1984), Holdren and Speyer (1987), Knauss and Copenhaver (1995), Lagache (1976), Manley and Evans (1986), Rafal'skiy et al. (1990), and Teng et al. (2001). Rate parameters are taken directly from Blum and Stillings (1995) for the acidic mechanism, and are regressed herein for the neutral mechanism from data (Table 14) in Helgeson et al. (1984) and for the basic mechanism from data (Table 14) in Bevan and Savage (1989), Blum and Stillings (1995), Gautier et al. (1994), Knauss & Copenhaver (1995). The derived rate parameters are summarized in Table 15.

Table 14. K-feldspar Dissolution rate Data.

an	ab	or	T, °C	[b]pH	[c]log k	Source
0	16	84	25	4	-8.65	Helgeson et al. 1984
0	16	84	50	4	-7.54	Helgeson et al. 1984
0	16	84	100	4	-5.76	Helgeson et al. 1984
0	16	84	150	4	-4.39	Helgeson et al. 1984
0	16	84	200	4	-3.3	Helgeson et al. 1984
0	16	84	250	4	-2.42	Helgeson et al. 1984
0	16	84	300	4	-1.69	Helgeson et al. 1984
0	16	84	350	4	-1.07	Helgeson et al. 1984
0	16	84	100	4	-6.2	Helgeson et al. 1984
0	16	84	150	4	-4.38	Helgeson et al. 1984
0	16	84	200	4	-3.52	Helgeson et al. 1984
0	16	84	200	4	-3.27	Helgeson et al. 1984
0	16	84	200	4	-3	Helgeson et al. 1984
0	16	84	250	5.58	-8.61	Helgeson et al. 1984
0	16	84	250	5.58	-2.42	Helgeson et al. 1984
0	16	84	200	5.64	-9.03	Helgeson et al. 1984
0	16	84	200	5.64	-3.3	Helgeson et al. 1984
0	16	84	300	5.65	-8.26	Helgeson et al. 1984
0	16	84	300	5.65	-1.69	Helgeson et al. 1984
0	16	84	150	5.82	-9.54	Helgeson et al. 1984
0	16	84	150	5.82	-4.39	Helgeson et al. 1984
0	16	84	350	5.91	-7.97	Helgeson et al. 1984
0	16	84	350	5.91	-1.07	Helgeson et al. 1984
0	16	84	25	6	-8.65	Helgeson et al. 1984
0	16	84	50	6	-7.54	Helgeson et al. 1984
0	16	84	100	6	-5.76	Helgeson et al. 1984
0	16	84	150	6	-4.39	Helgeson et al. 1984
0	16	84	200	6	-3.3	Helgeson et al. 1984
0	16	84	250	6	-2.42	Helgeson et al. 1984
0	16	84	300	6	-1.69	Helgeson et al. 1984
0	16	84	350	6	-1.07	Helgeson et al. 1984
0	16	84	100	6.13	-10.18	Helgeson et al. 1984
0	16	84	100	6.13	-5.76	Helgeson et al. 1984
0	16	84	50	6.64	-11.01	Helgeson et al. 1984
0	16	84	50	6.64	-7.54	Helgeson et al. 1984
0	16	84	25	7	-11.52	Helgeson et al. 1984
0	16	84	25	7	-8.65	Helgeson et al. 1984
0	16	84	150	8.94	-7.79	Gautier et al. 1994
0	16	84	150	8.94	-7.6	Gautier et al. 1994
--	--	97	300	9	-6.3	Alekseyev et al. 1997
--	--	97	300	9	-6.3	Alekseyev et al. 1997

[a]Composition

Table 14. K-feldspar Dissolution rate Data.

	[a]Composition		T, °C	[b]pH	[c]log k	Source
an	ab	or				
0	7	93	70	9	-12.03	Bevan and Savage 1989
0	7	93	95	9	-11.63	Bevan and Savage 1989
0	7	93	95	9	-11.72	Bevan and Savage 1989
0	6	95	70	9.51	-10.7	Knauss and Copenhaver 1995

a. -- = Not given.
b. Acid mechanism, pH 4-5.91; Neutral mechanism, pH 6-7; base mechanism, pH 8.94-13.
c. Log mole m^{-2} s^{-1}.

Table 15. K-Feldspar Dissolution Rate Parameters.

Acid Mechanism			Neutral Mechanism		Base Mechanism		
[a]log k	[b]E	[c]n	[a]log k	[b]E	[a]log k	[b]E	[c]n
-10.06	51.7	0.500	-12.41	38.0	-21.20	94.1	-0.823

a. Rate constant k computed from A and E, 25°C, pH = 0, mole m^{-2} s^{-1}.
b. Arrhenius activation energy E, kJ mole^{-1}.
c. Reaction order n with respect to H^{+}.

3.1.3 Feldspathoids: Nepheline and Leucite

Dissolution rate data for nepheline were evaluated from Brady and Walther (1989), Hamilton et al. (2001), Murphy and Helgeson (1989), Sverdrup (1990), and Tole et al. (1986), and for leucite, from Sverdrup (1990). Data for nepheline were selected from Tole et al. (1993) for the acidic and neutral mechanisms because they were obtained from experiments at a wider range of temperatures than the other references. The data from Tole et al. (1993) are summarized in Table 16, and the rate parameters determined by linear regression herein using eqns. (11) and (12) are given in Table 18. Rate parameters for the basic mechanism for nepheline and acidic, neutral, and basic mechanisms for leucite were compiled from Sverdrup (1990) and are summarized in Table 17, with activation energies calculated herein from reported rate constants at 8 and 25 °C; the results are also tabulated in Table 18.

Table 16. Nepheline Dissolution Rate Data.

T, °C	[a]pH	[b]log k	Source
25	3	-6.30	Tole et al. 1986
25	3	-6.30	Tole et al. 1986
60	3	-4.89	Tole et al. 1986
60	3	-4.89	Tole et al. 1986
80	3	-4.33	Tole et al. 1986
80	3	-4.33	Tole et al. 1986
25	5	-8.24	Tole et al. 1986
25	5	-8.24	Tole et al. 1986
60	5	-7.30	Tole et al. 1986
60	5	-7.30	Tole et al. 1986
80	5	-6.78	Tole et al. 1986
80	5	-6.78	Tole et al. 1986
25	7	-8.62	Tole et al. 1986
25	7	-8.62	Tole et al. 1986
60	7	-7.41	Tole et al. 1986
60	7	-7.41	Tole et al. 1986
80	7	-6.89	Tole et al. 1986
25	11	-8.56	Tole et al. 1986
60	11	-7.14	Tole et al. 1986

a. Acid mechanism, pH 3-5; Neutral mechanism, pH 7-11.
b. Log mole m^{-2} s^{-1}.

Table 17. Leucite Dissolution Rate Constants and Reaction Orders[a].

	Acid Mechanism			Neutral Mechanism		Base Mechanism		
	log $k_{8°C}$	log $k_{25°C}$	[b]n	log $k_{8°C}$	log $k_{25°C}$	log $k_{8°C}$	log $k_{25°C}$	[b]n
Leucite	-10.40	-9.0	0.700	-13.00	-12.2	-11.40	-10.8	-0.200

a. Data from Sverdrup, 1990; log k units, log mole m^{-2} s^{-1}.
b. Reaction order n with respect to H^+.

Table 18. Feldspathoid Dissolution Rate Parameters.

	Acid Mechanism			Neutral Mechanism		Base Mechanism		
	[a]log k	[b]E	[c]n	[a]log k	[b]E	[a]log k	[b]E	[c]n
Nepheline	-2.73	62.9	1.130	-8.56	65.4	-10.76	37.8	-0.200
Leucite	-6.00	132.2	0.700	-9.20	75.5	-10.66	56.6	-0.200

a. Rate constant k computed from A and E, 25°C, pH = 0, mole m^{-2} s^{-1}.
b. Arrhenius activation energy E, kJ $mole^{-1}$.
c. Reaction order n with respect to H^+.

3.2 Orthosilicates

3.2.1 Olivine Group

Dissolution rate data for olivine were evaluated from Awad et al. (2000), Bailey (1974), Blum and Lasaga (1986), Chen and Brantley (2000), Grandstaff (1986), Jonckbloedt (1998), Luce (1972), Murphy and Helgeson (1987; 1989), Oelkers (2001a), Pokrovsky and Schott (2000b), Pokrovsky and Schott (2000a), Rosso and Rimstidt (2000), Sverdrup (1990), Van Herk et al. (1989), Westrich et al. (1993), Wogelius and Walther, (1991), Wogelius and Walther (1992) and Xiao et al. (1999).

Dissolution rate data were selected for forsterite from Chen and Brantley (2000), Oelkers (2001a), Pokrovsky and Schott (2000b), Pokrovsky and Schott (2000a), and Wogelius and Walther (1992); these data are summarized in Table 19. The acidic mechanism for forsterite apparently operates at pH up to ~9, and there apparently is no basic mechanism. Rate parameters for the acidic and neutral mechanisms were regressed using eqn. (11), and the results are summarized in Table 20. Rate parameters for the acidic mechanism for fayalite is compiled from Sverdrup (1990; Table 20), with activation energies calculated herein from reported rate constants at 8 and 25 °C; for the neutral mechanism, a "cut-off" rate constant at 25 °C was calculated so that rates do not decrease with pH increasing above 9, and the activation energy is set equal to the acidic mechanism. The rate parameters for fayalite are also summarized in Table 20.

Table 19. Forsterite Dissolution Rate Data.

Composition	T, °C	[a]pH	[b]log k	Source
fo91	25	1.03	-7.23	Pokrovsky and Schott, 2000
fo91	25	1.11	-7.33	Pokrovsky and Schott, 2000
fo91	25	1.12	-7.28	Pokrovsky and Schott, 2000
fo91	65	1.8	-6.29	Wogelius and Walther, 1992
fo91	25	2	-7.80	Oelkers, 2001
fo91	25	2	-7.75	Oelkers, 2001
fo91	25	2	-7.92	Oelkers, 2001
fo91	25	2	-7.91	Oelkers, 2001
fo91	25	2	-7.85	Oelkers, 2001
fo91	25	2	-7.81	Oelkers, 2001
fo91	25	2	-7.98	Oelkers, 2001
fo91	25	2	-7.88	Oelkers, 2001
fo91	25	2	-7.88	Oelkers, 2001
fo91	25	2	-7.90	Oelkers, 2001
fo91	25	2	-7.89	Oelkers, 2001
fo91	25	2	-7.92	Oelkers, 2001
fo91	25	2	-7.90	Oelkers, 2001
fo91	25	2	-7.91	Oelkers, 2001

28

Table 19. Forsterite Dissolution Rate Data - continued.

Composition	T, °C	[a]pH	[b]log k	Source
fo91	25	2	-7.87	Oelkers, 2001
fo91	25	2	-7.93	Oelkers, 2001
fo91	25	2	-7.91	Oelkers, 2001
fo91	25	2	-7.93	Oelkers, 2001
fo91	25	2	-7.89	Oelkers, 2001
fo91	25	2	-7.99	Oelkers, 2001
fo91	25	2	-7.89	Oelkers, 2001
fo91	25	2	-7.92	Oelkers, 2001
fo91	35	2	-7.58	Oelkers, 2001
fo91	45	2	-7.03	Oelkers, 2001
fo91	55	2	-6.97	Oelkers, 2001
fo91	65	2	-6.09	Chen and Brantley, 2000
fo91	65	2	-6.57	Oelkers, 2001
fo91	25	2.13	-7.70	Pokrovsky and Schott, 2000
fo91	25	2.18	-7.71	Pokrovsky and Schott, 2000
fo91	25	2.21	-7.72	Pokrovsky and Schott, 2000
fo91	25	2.7	-7.73	Pokrovsky and Schott, 2000
fo91	25	2.74	-7.83	Pokrovsky and Schott, 2000
fo91	25	2.81	-7.82	Pokrovsky and Schott, 2000
fo91	25	2.82	-7.89	Pokrovsky and Schott, 2000
fo91	25	2.85	-8.30	Pokrovsky and Schott, 2000
f091	65	2.95	-6.76	Chen and Brantley, 2000
f091	65	2.95	-6.83	Chen and Brantley, 2000
f091	65	2.95	-6.85	Chen and Brantley, 2000
f091	65	2.95	-6.82	Chen and Brantley, 2000
fo91	65	2.95	-6.68	Chen and Brantley, 2000
fo91	25	2.99	-7.93	Pokrovsky and Schott, 2000
fo91	25	3.03	-7.97	Pokrovsky and Schott, 2000
fo91	25	3.05	-8.18	Pokrovsky and Schott, 2000
fo91	25	3.05	-8.28	Pokrovsky and Schott, 2000
fo91	25	3.08	-8.14	Pokrovsky and Schott, 2000
fo91	25	3.16	-8.25	Pokrovsky and Schott, 2000
fo91	25	3.26	-8.34	Pokrovsky and Schott, 2000
fo91	25	3.34	-8.55	Pokrovsky and Schott, 2000
fo91	25	3.6	-8.80	Pokrovsky and Schott, 2000
f091	65	4	-7.60	Chen and Brantley, 2000
fo91	25	4.15	-9.03	Pokrovsky and Schott, 2000
fo91	25	4.2	-8.69	Pokrovsky and Schott, 2000
fo91	25	4.22	-8.78	Pokrovsky and Schott, 2000
fo91	25	4.41	-8.80	Pokrovsky and Schott, 2000
fo91	25	4.49	-8.98	Pokrovsky and Schott, 2000

Table 19. Forsterite Dissolution Rate Data - continued.

Composition	T, °C	[a]pH	[b]log k	Source
fo91	25	4.55	-9.03	Pokrovsky and Schott, 2000
fo91	25	4.77	-8.98	Pokrovsky and Schott, 2000
fo91	25	4.85	-9.02	Pokrovsky and Schott, 2000
fo91	25	4.95	-9.15	Pokrovsky and Schott, 2000
f091	65	5	-7.92	Chen and Brantley, 2000
fo91	25	5.4	-9.31	Pokrovsky and Schott, 2000
fo91	25	5.44	-9.47	Pokrovsky and Schott, 2000
fo91	25	5.44	-9.47	Pokrovsky and Schott, 2000
fo91	25	5.47	-9.57	Pokrovsky and Schott, 2000
fo91	25	5.61	-9.79	Pokrovsky and Schott, 2000
fo91	25	5.7	-9.49	Pokrovsky and Schott, 2000
fo91	65	6	-8.13	Wogelius/Walther, 1992
fo91	25	6.13	-9.92	Pokrovsky and Schott, 2000
fo91	25	6.18	-9.60	Pokrovsky and Schott, 2000
fo91	25	6.28	-9.72	Pokrovsky and Schott, 2000
fo91	25	6.39	-10.04	Pokrovsky and Schott, 2000
fo91	25	6.6	-9.97	Pokrovsky and Schott, 2000
fo91	25	7.19	-10.11	Pokrovsky and Schott, 2000
fo91	25	7.21	-10.04	Pokrovsky and Schott, 2000
fo91	25	7.25	-9.88	Pokrovsky and Schott, 2000
fo91	25	7.33	-9.93	Pokrovsky and Schott, 2000
fo91	25	7.6	-10.47	Pokrovsky and Schott, 2000
fo91	25	7.9	-10.57	Pokrovsky and Schott, 2000
fo91	25	7.98	-10.39	Pokrovsky and Schott, 2000
fo91	25	8.02	-10.13	Pokrovsky and Schott, 2000
fo91	25	8.13	-10.33	Pokrovsky and Schott, 2000
fo91	25	8.38	-10.18	Pokrovsky and Schott, 2000
fo91	25	8.5	-10.33	Pokrovsky and Schott, 2000
fo91	25	8.53	-10.17	Pokrovsky and Schott, 2000
fo91	25	8.55	-10.42	Pokrovsky and Schott, 2000
fo91	25	8.55	-10.40	Pokrovsky and Schott, 2000
fo91	25	8.63	-10.44	Pokrovsky and Schott, 2000
fo91	25	8.68	-10.46	Pokrovsky and Schott, 2000
fo91	25	8.71	-10.60	Pokrovsky and Schott, 2000
fo91	25	9.3	-10.49	Pokrovsky and Schott, 2000
fo91	25	9.58	-10.54	Pokrovsky and Schott, 2000
fo91	25	10.08	-10.79	Pokrovsky and Schott, 2000
fo91	25	10.24	-10.72	Pokrovsky and Schott, 2000
fo91	25	10.76	-10.38	Pokrovsky and Schott, 2000
fo91	25	10.78	-10.95	Pokrovsky and Schott, 2000
fo91	25	10.85	-10.31	Pokrovsky and Schott, 2000

Table 19. Forsterite Dissolution Rate Data - continued.

Composition	T, °C	[a]pH	[b]log k	Source
fo91	25	10.9	-10.44	Pokrovsky and Schott, 2000
fo91	25	10.9	-10.69	Pokrovsky and Schott, 2000
fo91	25	10.95	-10.60	Pokrovsky and Schott, 2000
fo91	25	11.01	-10.57	Pokrovsky and Schott, 2000
fo91	25	11.1	-10.65	Pokrovsky and Schott, 2000
fo91	25	11.11	-10.56	Pokrovsky and Schott, 2000
fo91	25	11.12	-10.52	Pokrovsky and Schott, 2000
fo91	25	11.13	-10.71	Pokrovsky and Schott, 2000
fo91	25	11.15	-10.57	Pokrovsky and Schott, 2000
fo91	25	12.06	-10.85	Pokrovsky and Schott, 2000

a. Acid mechanism, pH 1.03-8.71; Neutral mechanism, pH 9.3-12.06.
b. Log mole m^{-2} s^{-1}.

Table 20. Orthosilicate Dissolution Rate Constants and Reaction Orders[a].

	Acid Mechanism			Neutral Mechanism		Base Mechanism		
	log $k_{8°C}$	log $k_{25°C}$	[b]n	log $k_{8°C}$	log $k_{25°C}$	log $k_{8°C}$	log $k_{25°C}$	[b]n
Fayalite	-5.8	-4.8	1.0	--	--	--	--	--
Almandine	-6.2	-5.2	1.0	-11.8	-10.7	-9.1	-8.7	-0.3
Grossular	-6	-5.1	1.0	-11.8	-10.7	--	--	--
Andradite	-6.2	-5.2	1.0	-11.8	-10.7	--	--	--
Staurolite	-7.1	-6.9	1.0	-12.8	-12.2	-11.1	-10.6	-0.3
Zoisite	-8.2	-7.5	0.5	--	--	--	--	--

a. Data from Sverdrup, 1990; log k units, log mole m^{-2} s^{-1}.
b. Reaction order n with respect to H^{+}.

3.2.2 Garnet Group

Rate parameters for the acidic, neutral, and basic mechanisms for almandine, and acidic and neutral mechanisms (data are absent for the basic mechanism) for grossular and andradite are compiled from Sverdrup (1990; Table 20), with activation energies calculated herein from reported rate constants at 8 and 25 °C. The rate parameters for the garnet group minerals are summarized in Table 22.

3.2.3 Al$_2$SiO$_5$ Group

Dissolution rate data for kyanite were obtained from Oelkers and Schott (1999; Table 21) for the acidic mechanism only. The rate parameters are regressed herein using eqn. (11), and are summarized in Table 23. For the neutral mechanism, a "cut-off" rate constant at 25 °C was calculated so that rates do not decrease with pH increasing above 7, and the activation energy is set equal to that for the acidic mechanism.

Table 21. Kyanite Dissolution Rate Data.

T, °C	pH	[a]log k	T, °C	pH	[a]log k
150	1.65	-9.63	150	2.04	-9.87
150	1.65	-9.55	150	2.04	-9.87
150	1.65	-9.42	150	2.04	-9.86
150	1.85	-9.84	150	2.04	-9.79
150	1.85	-9.66	150	2.04	-9.88
150	1.85	-9.65	150	2.04	-9.79
108	2.03	-10.96	150	2.04	-9.82
108	2.03	-10.96	131	2.04	-9.98
111	2.03	-10.54	174	2.06	-9.89
113	2.03	-10.28	175	2.06	-9.67
121	2.03	-10.48	175	2.06	-9.69
121	2.03	-10.48	175	2.06	-9.62
121	2.03	-10.66	175	2.06	-9.69
122	2.03	-10.48	175	2.06	-9.61
125	2.03	-10.40	175	2.06	-9.56
125	2.03	-10.34	175	2.06	-9.77
125	2.03	-10.28	194	2.07	-9.46
126	2.03	-10.40	194	2.07	-9.27
126	2.03	-10.29	150	2.24	-10.40
150	2.04	-9.86	150	2.24	-10.24
150	2.04	-9.92	150	2.24	-10.21
150	2.04	-9.84	150	2.24	-10.37

a. Log mole m^{-2} s^{-1}.

3.2.4 Staurolite

Rate parameters for the acidic, neutral, and basic mechanisms for staurolite were compiled from Sverdrup (1990; Table 20), with activation energies calculated herein from reported rate constants at 8 and 25 °C. The rate parameters for the staurolite are summarized in Table 23.

3.2.5 Epidote Group

Dissolution rate data for epidote and zoisite were evaluated from Rose (1991), Kalinowski et al. (1998), and Sverdrup (1990). Data for the acidic, neutral, and basic mechanisms for epidote from Rose (1991), and Kalinowski et al. (1998) were selected, and are tabulated in Table 22. The rate parameters for epidote are regressed herein using eqn. (11), and are summarized in Table 23. Rate parameters for the acidic mechanism for zoisite was compiled from Sverdrup (1990; Table 20), with the activation energy calculated herein from reported rate constants at 8 and 25 °C; for the neutral mechanism, a "cut-off" rate constant at 25 °C was calculated so that rates do not decrease with pH increasing above 7, and the activation energy is set equal to the acidic mechanism. The rate parameters for zoisite are summarized in Table 23.

Table 22. Epidote Dissolution Rate Data.

T, °C	[a]pH	[b]log k	Source
25	0.2	-10.23	Kalinowski et al. 1998
25	1.08	-10.49	Kalinowski et al. 1998
25	1.29	-11.31	Kalinowski et al. 1998
90	1.29	-8.715	Rose 1991
25	1.4	-11.53	Kalinowski et al. 1998
25	1.4	-11.528	Rose 1991
50	1.4	-10.322	Rose 1991
70	1.4	-9.268	Rose 1991
70	1.4	-9.63	Rose 1991
70	1.4	-9.677	Rose 1991
90	1.4	-8.9	Rose 1991
25	1.99	-11.19	Kalinowski et al. 1998
25	2.01	-10.73	Kalinowski et al. 1998
25	2.5	-11.8	Kalinowski et al. 1998
90	2.5	-9.2	Rose 1991
90	2.5	-9.269	Rose 1991
25	2.98	-11.36	Kalinowski et al. 1998
25	2.99	-11.63	Kalinowski et al. 1998
25	3	-11.64	Kalinowski et al. 1998
25	3.03	-11.42	Kalinowski et al. 1998
25	3.47	-12.02	Kalinowski et al. 1998
90	3.47	-9.424	Rose 1991
90	3.47	-9.424	Rose 1991
90	3.47	-9.528	Rose 1991
25	4.02	-12.19	Kalinowski et al. 1998
25	4.05	-11.72	Kalinowski et al. 1998
25	4.05	-12	Kalinowski et al. 1998
25	4.12	-11.65	Kalinowski et al. 1998
25	4.38	-12.17	Kalinowski et al. 1998
90	4.38	-9.578	Rose 1991
25	5.5	-12.15	Kalinowski et al. 1998
90	5.5	-9.55	Rose 1991
25	5.6	-11.8	Kalinowski et al. 1998
25	6.48	-12.29	Kalinowski et al. 1998
25	6.5	-11.93	Kalinowski et al. 1998
90	6.62	-9.795	Rose 1991
90	7.75	-9.892	Rose 1991
90	8.64	-10.048	Rose 1991
90	10.83	-8.831	Rose 1991
25	10.6	-11.44	Kalinowski et al. 1998

a. Acid mechanism, pH 1.2 – 4.38; Neutral mechanism, pH 5.5-7.75; basic
mechanism, 8.64-10.8.
b. Log mole m^{-2} s^{-1}.

Table 23. Orthosilicate Dissolution Rate Parameters.

	Acid Mechanism			Neutral Mechanism		Base Mechanism		
	[a]log k	[b]E	[c]n	[a]log k	[b]E	[a]log k	[b]E	[c]n
Forsterite	-6.85	67.2	0.470	-10.64	79.0	--	--	--
Fayalite	-4.80	94.4		-12.80	94.4	--	--	--
Almandine	-5.20	94.4	1.000	-10.70	103.8	-13.71	37.8	-0.350
Grossular	-5.10	85.0	1.000	-10.70	103.8	--	--	--
Andradite	-5.20	94.4	1.000	-10.70	103.8	--	--	--
Kyanite	-10.17	-53.9	1.268	-17.44	53.9	--	--	--
Staurolite	-6.90	18.9	1.000	-12.20	56.6	-14.90	47.2	-0.300
Epidote	-10.60	71.1	0.338	-11.99	70.7	-17.33	79.1	-0.556
Zoisite	-7.50	66.1	0.500	-11.20	66.1	--	--	--

a. Rate constant k computed from A and E, 25°C, pH = 0, mole m^{-2} s^{-1}.
b. Arrhenius activation energy E, kJ $mole^{-1}$.
c. Reaction order n with respect to H^+.

3.3 Cyclosilicates

3.3.1 Cordierite and Tourmaline

Rate parameters for the acidic and neutral mechanisms (data are absent for the basic mechanism) for cordierite and tourmaline were compiled from Sverdrup (1990; Table 24), with activation energies calculated herein from reported rate constants at 8 and 25 °C. The rate parameters for the garnet group minerals are summarized in Table 22.

Table 24. Cyclosilicate Dissolution Rate Constants and Reaction Orders[a].

	Acid Mechanism			Neutral Mechanism	
	log $k_{8°C}$	log $k_{25°C}$	[b]n	log $k_{8°C}$	log $k_{25°C}$
Cordierite	-5.0	-3.8	1.000	-11.5	-11.2
Tourmaline	-7.3	-6.5	1.000	-12.1	-11.2

a. Data from Sverdrup, 1990; log k units, log mole m^{-2} s^{-1}.
b. Reaction order n with respect to H^+.

Table 25. Cyclosilicate Dissolution Rate Parameters.

	Acid Mechanism			Neutral Mechanism	
	[a]log k	[b]E	[c]n	[a]log k	[b]E
Cordierite	-3.80	113.3	1.000	-11.20	28.3
Tourmaline	-6.50	75.5	1.000	-11.20	85.0

a. Rate constant k computed from A and E, 25°C, pH = 0, mole m^{-2} s^{-1}.
b. Arrhenius activation energy E, kJ $mole^{-1}$.
c. Reaction order n with respect to H^+.

3.4 Inosilicates

3.4.1 Pyroxene Group / Pyroxenoid Group

Dissolution rate data for pyroxenes and pyroxenoids were evaluated from Bailey (1974), Brantley and Chen (1995), Chen and Brantley (1998), Knauss et al. (1993), Murphy and Helgeson (1987; 1989), Rimstidt and Dove (1986), Schott and Berner (1985), Schott et al. (1981), Siegel and Pfannkuch (1984), Sverdrup (1990), and Weissbart (2000).

Dissolution rate data for the acidic and neutral mechanisms (data are absent for the basic mechanism) were selected as follows: augite, from Schott et al. (1981) and Sverdrup (1990); bronzite, from Sverdrup (1990); diopside, from Brantley and Chen (1995), Chen and Brantley (1998), Knauss et al. (1993), and Schott and Berner (1985); enstatite, from Schott and Berner (1985); jadeite, from Sverdrup (1990); spodumene, from Sverdrup (1990); wollastonite, from Murphy and Helgeson (1987; 1989) and Rimstidt and Dove (1986). The rate parameters were regressed using eqn. (11), except for the bronzite data from Sverdrup (1990), for which rate constants at 8 and 25 °C for single mechanisms are used herein to calculate the activation energy. The resulting rate parameters are summarized in Table 26.

For enstatite and augite, the available data are limited to pH less than ~7. Although rates may decrease further with further pH increase above 7, a "cut-off" rate constant at 25 °C was calculated for the neutral mechanism so that rates do not decrease with pH increasing above 7, and the activation energy is set equal to the acidic mechanism.

Table 26. Pyroxene and Pyroxenoid Dissolution Rate Parameters.

	Acid Mechanism				Neutral Mechanism	
	[a]log k	[b]E	[c]n		[a]log k	[b]E
augite	-6.82	78.0	0.700		-11.97	78.0
bronzite	-8.30	47.2	0.650		-11.70	66.1
diopside	-6.36	96.1	0.710		-11.11	40.6
enstatite	-9.02	80.0	0.600		-12.72	80.0
jadeite	-6.00	132.2	0.700		-9.50	94.4
spodumene	-4.60	94.4	0.700		-9.30	66.1
wollastonite	-5.37	54.7	0.400		-8.88	54.7

a. Rate constant k computed from A and E, 25°C, pH = 0, mole m^{-2} s^{-1}.
b. Arrhenius activation energy E, kJ mole^{-1}.
c. Reaction order n with respect to H$^+$.

3.4.2 Amphibole Group

Dissolution rate data for amphiboles were evaluated from Brantley and Chen (1995), Chen and Brantley (1998), Sverdrup (1990), and Zhang and Bloom (1999). Data for the acidic and neutral mechanisms (data are absent for the basic mechanism) were selected as follows: anthophyllite, from Chen and Brantley (1998); glaucophane, hornblende, riebeckite and tremolite, from Sverdrup (1990). The rate parameters were regressed using eqn. (11), except for the data from Sverdrup (1990), for which rate constants at 8 and 25 °C for single mechanisms are used herein to calculate the activation energy. The resulting rate parameters are summarized in Table 27.

Table 27. Amphibole Dissolution Rate Parameters.

	Acid Mechanism				Neutral Mechanism	
	[a]log k	[b]E	[c]n		[a]log k	[b]E
anthophyllite	-11.94	51.0	0.440		-14.24	51.0
glaucophane	-5.60	85.0	0.700		-10.10	94.4
hornblende	-7.00	75.5	0.600		-10.30	94.4
riebeckite	-7.70	56.6	0.700		-12.20	47.2
tremolite	-8.40	18.9	0.700		-10.60	94.4

a. Rate constant k computed from A and E, 25°C, pH = 0, mole m^{-2} s^{-1}.
b. Arrhenius activation energy E, kJ mole^{-1}.
c. Reaction order n with respect to H$^+$.

3.5 Phyllosilicates

3.5.1 Mica Group

Dissolution rate data for the micas were evaluated from Acker and Bricker (1992), Clemency and Lin (1981), Kalinowski and Schweda (1996), Knauss and Wolery (1989), Kuwahara and Aoke (1999), Lin and Clemency (1981a; 1981b), Malmstrom and Banwart (1997), Nagy (1995), Robie (1976), Sverdrup (1990), Swoboda-Colberg and Drever (1993), Taylor et al. (2000b), and Trotignon and Turpault (1992).

Data were selected as follows: biotite, from Acker and Bricker (1992) and Nagy (1995); glauconite, from Sverdrup (1990); muscovite, paragonite, phlogopite and pyrophyllite, from Nagy (1995). The rate parameters were regressed using eqn. (11), except for the data from Sverdrup (1990), for which rate constants at 8 and 25 °C for single mechanisms are used herein to calculate the activation energy. The compiled rate parameters are summarized in Table 28.

Table 28. Orthosilicate Dissolution Rate Parameters.

	Acid Mechanism			Neutral Mechanism		Base Mechanism		
	[a]log k	[b]E	[c]n	[a]log k	[b]E	[a]log k	[b]E	[c]n
biotite	-9.84	22.0	0.525	-12.55	22.0	--	--	--
glauconite	-4.80	85.0	0.700	-9.10	85.0	--	--	--
muscovite	-11.85	22.0	0.370	-13.55	22.0	-14.55	22.0	-0.220
muscovite	--	--	--	-13.00	22.0	--	--	--
paragonite	--	--	--	-13.00	22.0	--	--	--
phlogopite	--	--	--	-12.40	29.0	--	--	--
pyrophyllite	--	--	--	-12.40	29.0	--	--	--

a. Rate constant k computed from A and E, 25°C, pH = 0, mole m^{-2} s^{-1}.
b. Arrhenius activation energy E, kJ $mole^{-1}$.
c. Reaction order n with respect to H^+.

3.5.2 Clay Group

Dissolution rate data for three additional clay group minerals were evaluated: kaolinite (Bauer and Berger, 1998; Cama et al., 2002; Carroll and Walther, 1990; Carroll-Webb and Walther, 1988; Devidal et al., 1997; Ganor et al., 1995; Hayashi and Yamada, 1990; Huertas et al., 1999a; Huertas et al., 2001b; Huertas et al., 1999b; Metz and Ganor, 2001; Nagy, 1995; Nagy et al., 1991; Nagy and Lasaga, 1990; Nagy and Lasaga, 1993; Oelkers et al., 2001; Polzer and Hem, 1965; Soong, 1993; Soong and Barnes, 1991; Sutheimer et al., 1999; Wieland and Stumm, 1992); montmorillonite (Furrer et al., 1993; Hayashi and Yamada, 1990; Huertas et al., 2001a; Nagy, 1995; Zysset and Schindler, 1996); and smectite (Altaner, 1986; Bauer and Berger, 1998; Cama et al., 2000; Cama et al., 1994; Novák and Cícel, 1978).

Data for the clay group minerals were selected as follows: kaolinite, from Carroll and Walther (1990), Ganor et al. (1995), Huertas et al. (1999a), Huertas et al. (1999b), Nagy et al. (1991), Soong (1993); montmorillonite, from Nagy (1995); smectite, from Bauer and Berger

(1998), Huertas et al. (2001a), Sverdrup (1990), and Zysset and Schindler (1996). The rate parameters were regressed using eqn. (11), except for the data from Sverdrup (1990), for which rate constants at 8 and 25 °C for single mechanisms are used herein to calculate the activation energy. The compiled rate parameters are summarized in Table 29. Nagy et al. (1991) have quantified the chemical affinity parameters for kaolinite at 80 °C and pH = 3; with the experimental uncertainty, the experimental data can be fit to eqn. (4) with either p = 1.000 and q = 0.897, or p = 0.850 and q = 1.000.

Table 29. Clay Group Mineral Dissolution Rate Parameters.

	Acid Mechanism			Neutral Mechanism			Base Mechanism		
	[a]log k	[b]E	[c]n	[a]log k	[b]E		[a]log k	[b]E	[c]n
kaolinite	-11.31	65.9	0.777	-13.18	22.2		-17.05	17.9	-0.472
[d]montmorillonite	-12.71	48.0	0.220	-14.41	48.0		-14.41	48.	-0.130
[e]smecite	-10.98	23.6	0.340	-12.78	35.0		-16.52	58.9	-0.400

a. Rate constant k computed from A and E, 25°C, pH = 0, mole m^{-2} s^{-1}.
b. Arrhenius activation energy E, kJ $mole^{-1}$.
c. Reaction order n with respect to H^+.
d. Montmorillonite, $K_{0.318}(Si_{3.975}Al_{0.025})(Al_{1.509}Fe_{0.205}Mg_{0.283})(OH)_2$.
e. Smectite, $K_{0.04}Ca_{0.5}(Al_{2.8}Fe_{0.53}Mg_{0.7})(Si_{7.65}Al_{0.35})O_{20}(OH)_4$.

3.5.3 Miscellaneous Phyllosilicates

Dissolution rate data for several miscellaneous phyllosilicate minerals were evaluated: serpentine (Bales and Morgan, 1985; Cetisli and Gedikbey, 1990; Gronow, 1987; Hume and Rimstidt, 1992; Lin and Clemency, 1981b; Nagy, 1995; Sverdrup, 1990; Thomassin et al., 1977), chlorite (Hayashi and Yamada, 1990; Johnson et al., 2001; Nagy, 1995; Sverdrup, 1990), talc (Lin and Clemency, 1981b; Nagy, 1995), and prehnite (Rose, 1991).

Data for these phyllosilicate minerals were selected as follows: lizardite serpentine, from Sverdrup (1990); chrysotile serpentine, from Nagy (1995); chlorite, from Nagy (1995); talc, from Nagy (1995); and prehnite, from Rose (1991). The compiled parameters are summarized in Table 30.

Table 30. Miscellaneous Phyllosilicate Mineral Dissolution Rate Parameters.

	Acid Mechanism			Neutral Mechanism		Base Mechanism		
	[a]log k	[b]E	[c]n	[a]log k	[b]E	[a]log k	[b]E	[c]n
lizardite	-5.70	75.5	0.800	-12.40	56.6	--	--	--
chrysotile	--	--	--	-12.00	73.5	-13.58	73.5	-0.230
[d]chlorite	-11.11	88.0	0.500	-12.52	88.0	--	--	--
talc	--	--	--	-12.00	42.0	--	--	--
prehnite	-10.66	80.5	0.256	-13.16	93.4	-14.86	93.4	-0.200

a. Rate constant k computed from A and E, 25°C, pH = 0, mole m^{-2} s^{-1}.
b. Arrhenius activation energy E, kJ $mole^{-1}$.
c. Reaction order n with respect to H^+.
d. Clinochlore 14 Å.

3.6 Oxides

Dissolution rate data for several oxide minerals were evaluated: goethite (Ruan and Gilkes, 1995), hematite (Bruno and Duro, 2000; Bruno et al., 1992; Hummel, 2000; Petrie, 1995; Ruan and Gilkes, 1995), ilmenite (White et al., 1994), magnetite (White et al., 1994), manganite (Petrie, 1995), pyrolusite (Petrie, 1995), and uraninite (Grandstaff, 1976). Data for the oxide minerals were selected as follows: goethite, from Ruan and Gilkes (1995); hematite, Ruan and Gilkes (1995); ilmenite, White et al. (1994); magnetite, White et al. (1994); pyrolusite, Petrie (1995); and uraninite Grandstaff (1976). The compiled parameters are summarized in Table 31.

Table 31. Oxide Mineral Dissolution Rate Parameters.

	Acid Mechanism			Neutral Mechanism	
	[a]log k	[b]E	[c]n	[a]log k	[b]E
goethite	--	--	--	-7.94	86.5
hematite	-9.39	66.2	1.000	-14.60	66.2
magnetite	-8.59	18.6	0.279	-10.78	18.6
ilmenite	-8.35	37.9	0.421	-11.16	37.9
uraninite	--	--	--	-7.98	32.0

a. Rate constant k computed from A and E, 25°C, pH = 0, mole m^{-2} s^{-1}.
b. Arrhenius activation energy E, kJ $mole^{-1}$.
c. Reaction order n with respect to H^+.

3.7 Hydroxides

Dissolution rate data for brucite (Jordan and Rammensee, 1996; Lin and Clemency, 1981b; Nagy, 1995; Sverdrup, 1990), gibbsite (Bloom, 1983; Bloom and Erich, 1987; Chang et al., 1979; Ganor et al., 1999; Mogollón et al., 1996; Mogollón et al., 2000; Nagy, 1995; Nagy and Lasaga, 1990; Nagy and Lasaga, 1992; Nagy and Lasaga, 1993; Packter and Dhillon, 1974; Scotford and Glastonbury, 1972a; Scotford and Glastonbury, 1972b), and diaspore (Chang et al., 1979) were evaluated. Data for brucite were selected from Nagy (1995) and Jordan and Rammensee (1996). Data for gibbsite were selected from Nagy and Lasaga (1992) and Packter and Dhillon (1974). The compiled parameters are summarized in Table 32.

Table 32. Hydroxide Mineral Dissolution Rate Parameters.

	Acid Mechanism			Neutral Mechanism		Base Mechanism		
	[a]log k	[b]E	[c]n	[a]log k	[b]E	[a]log k	[b]E	[c]n
brucite	-4.73	59.0	0.500	-8.24	42.0	--	--	--
gibbsite	-7.65	47.5	0.992	-11.50	61.2	-16.65	80.1	-0.784
diaspore	--	--	--	-13.33	47.5	-23.60	47.5	-1.503

a. Rate constant k computed from A and E, 25°C, pH = 0, mole m^{-2} s^{-1}.
b. Arrhenius activation energy E, kJ $mole^{-1}$.
c. Reaction order n with respect to H^+.

3.8 Carbonates

Dissolution rate data for four carbonate minerals were evaluated: calcite (Alkattan et al., 1998; Alkattan et al., 2002; Berner and Morse, 1974; Brown et al., 1993; Busenberg and Plummer, 1986; Chou et al., 1989; Deleuze and Brantley, 1997; House, 1981; Inskeep and Bloom, 1985; Jeschke and Dreybrodt, 2002b; Jiménez-López et al., 2001; Jordan and Rammensee, 1998; Lebrón and Suárez, 1996; Lebrón and Suárez, 1998; MacInnis and Brantley, 1992; Maldonado et al., 1992; Morse, 1978; Mucci, 1986; Mucci and Morse, 1983; Plummer and Wigley, 1976; Plummer et al., 1978; Plummer et al., 1979; Reddy, 1986; Reddy and Gaillard, 1981; Reddy et al., 1981; Schott et al., 1989; Shiraki and Brantley, 1995; Sjöberg, 1976; Sjöberg and Rickard, 1983; Sjöberg and Rickard, 1984a; Sjöberg and Rickard, 1984b; Sjöberg and Rickard, 1985; Talman et al., 1990; Teng et al., 2000; Zhang and Dawe, 1998; Zhang and Dawe, 2000; Zhong and Mucci, 1989; Zhong and Mucci, 1993; Zuddas and Mucci, 1994; Zuddas and Mucci, 1998); dawsonite (Johnson et al., 2001); dolomite (Arvidson and Mackenzie, 1999; Baker and Kastner, 1981a; Baker and Kastner, 1981b; Busenberg and Plummer, 1982; Busenberg and Plummer, 1986; Chou et al., 1989; Gaines, 1980; Gautelier et al., 1999; Katz and Matthews, 1977; Lüttge et al., 2003; Nordeng and Sibley, 1994; Sibley et al., 1987); magnesite (Chou et al., 1989; Higgins et al., 2002; Johnson et al., 2001; Jordan et al., 2001; Pokrovsky and Schott, 1999); and siderite (Greenberg and Tomson, 1992; Jensen et al., 2002).

Data for the carbonate minerals were selected as follows: calcite, from Plummer et al. (1978) and Talman et al. (1990); dawsonite, Johnson et al. (2001); dolomite, Busenberg and

Plummer (1982); and magnesite, Chou et al. (1989) and Pokrovsky and Schott (1999). The rate parameters were regressed using eqn. (11), and are summarized in Table 33. In the absence of data for the activation energy for magnesite dissolution, the activation energy of calcite is assigned to magnesite. Pokrovsky and Schott (1999) have quantified the chemical affinity parameters for magnesite at 25 °C with pH ranging from 0.2 to 12, with $p = 4.00$ and $q = 1.00$.

Table 33. Carbonate Mineral Dissolution Rate Parameters.

	Acid Mechanism			Neutral Mechanism		Carbonate Mechanism		
	[a]log k	[b]E	[c]n	[a]log k	[b]E	[a]log k	[b]E	[d]n
calcite	-0.30	14.4	1.000	-5.81	23.5	-3.48	35.4	1.000
dawsonite	--	--	--	-7.00	62.8	--	--	--
[e]dolomite	-3.19	36.1	0.500	-7.53	52.2	-5.11	34.8	0.500
[f]dolomite	-3.76	56.7	0.500	-8.60	95.3	-5.37	45.7	0.500
magnesite	-6.38	14.4	1.000	-9.34	23.5	-5.22	62.8	1.000

a. Rate constant k computed from A and E, 25°C, pH = 0, mole m^{-2} s^{-1}.
b. Arrhenius activation energy E, kJ $mole^{-1}$.
c. Reaction order n with respect to H^+.
d. Reaction order n with respect to $P(CO_2)$.
e. Sedimentary (disordered) dolomite.
f. Hydrothermal (ordered) dolomite.

3.9 Sulfates

Dissolution rate data for several sulfate minerals were evaluated: anhydrite (Barton and Wilde, 1971; Bildstein et al., 2001; Dove and Czank, 1995; Jeschke and Dreybrodt, 2002b); anglesite (Dove and Czank, 1995); barite (Christy and Putnis, 1993; Dove and Czank, 1995; Kornicker et al., 1991); celestite (Dove and Czank, 1995); and gypsum (Jeschke et al., 2001; Raines and Dewers, 1997). Data for the sulfate minerals were selected as follows: anhydrite, from Barton and Wilde (1971) and Dove and Czank (1995); anglesite, barite and celestite, from Dove and Czank (1995); and gypsum, from Raines and Dewers (1997). The rate parameters were regressed using eqn. (11), and are summarized in Table 34. Date were insufficient to calculate activation energies for the neutral mechanism for gypsum, and the acidic mechanisms for anglesite and barite; activation energies for the neutral mechanisms for anglesite and barite are assigned to the respective acidic mechanisms. The acidic mechanism for celestite apparently extends to alkaline pH, and there is no evident neutral mechanism.

Table 34. Sulfate Mineral Dissolution Rate Parameters.

	Acid Mechanism				Neutral Mechanism	
	[a]log k	[b]E	[c]n		[a]log k	[b]E
anglesite	-5.58	31.3	0.298		-6.50	31.3
anhydrite	--	--	--		-3.19	14.3
gypsum	--	--	--		-2.79	0
barite	-6.90	30.8	0.220		-7.90	30.8
celestite	-5.66	23.8	0.109		--	--

a. Rate constant k computed from A and E, 25°C, pH = 0, mole m^{-2} s^{-1}.
b. Arrhenius activation energy E, kJ mole^{-1}.
c. Reaction order n with respect to H$^+$.

3.10 Sulfides

Dissolution rate data for several sulfide minerals were evaluated: AsS, amorphous (Lengke and Tempel, 2003); As$_2$S$_3$, amorphous (Lengke and Tempel, 2001); Orpiment and As$_2$S$_3$, amorphous (Lengke and Tempel, 2002); pyrite (Gibbs et al., 1997a; Gibbs et al., 1997b; Holmes and Crundwell, 2000; Kamei and Ohmoto, 2000; Lennie and Vaughan, 1992; McKibben and Barnes, 1986; Moses and Herman, 1991; Moses et al., 1987; Nicholson et al., 1988; Nicholson et al., 1990; Rickard, 1997; Rickard and Luther, 1997; Rickard, 1975; Rimstidt and Vaughan, 2003; Schoonen and Barnes, 1991a; Schoonen and Barnes, 1991b; Schoonen and Barnes, 1991c; Wiersma and Rimstidt, 1984; Williamson and Rimstidt, 1994); pyrrhotite (Dekkers and Schoonen, 1994; Janzen et al., 2000; Thomas et al., 2001); Realgar (Lengke and Tempel, 2003); and Sphalerite (Weisener et al., 2003).

Data for the sulfide minerals were selected as follows: As$_2$S$_3$, amorphous, from Lengke and Tempel (2001); pyrite, from McKibben and Barnes (1986); and pyrrhotite, from Janzen et al. (2000). The rate parameters were regressed using eqn. (11) or compiled directly from the references, and are summarized in Table 35.

Table 35. Sulfide Mineral Dissolution Rate Parameters.

	Acid Mechanism				Neutral Mechanism			Base Mechanism		
	[a]log k	[b]E	[c]n	[d]n	[a]log k	[b]E	[e]n	[a]log k	[b]E	[c]n
pyrite	-7.52	56.9	-0.500	0.500	-4.55	56.9	0.500	--	--	--
[f]pyrrhotite	-8.04	50.8	-0.597	0.355	--	--	--	--	--	--
[g]pyrrhotite	-6.79	63.0	-0.090	0.356	--	--	--	--	--	--
[h]As$_2$S$_3$	--	--	--	--	-9.83	8.7	0.180	-17.39	8.7	-1.208

a. Rate constant k computed from A and E, 25°C, pH = 0, mole m^{-2} s^{-1}.
b. Arrhenius activation energy E, kJ mole^{-1}.
c. Reaction order n with respect to H$^+$.
d. Reaction order n with respect to Fe^{+++}.
e. Reaction order n with respect to O$_2$.
f. Monoclinic pyrrhotite.
g. Hexagonal pyrrhotite.
h. Amorphous As$_2$S$_3$.

3.11 Phosphates

Dissolution rate data for apatite from several references were evaluated (Chien, 1977; Chien et al., 1980; Christoffersen et al., 1978; Fawzi et al., 1978; Fox et al., 1978; Guidry and Mackenzie, 2003; Hull and Hull, 1987; Valsami-Jones et al., 1998). Data for hydroxyapatite and fluorapaite were selected from Fawzi et al. (1978) and Valsami-Jones et al. (1998). The rate parameters were regressed using eqn. (11), and are summarized in Table 36. For the neutral mechanism, a "cut-off" rate constant at 25 °C was calculated so that rates do not decrease with pH increasing above 7, and the activation energy is set equal to the acidic mechanism. The uncertainty in activation energy may be quite large because it was computed from dissolution rates obtained from experiments with minimal temperature difference, 25 and 28 °C (Fawzi et al., 1978); these data were for experiments with hydroxyapatite, and the tabulated activation energy for fluorapatite dissolution is taken equal to that of hydroxyapatite.

Table 36. Phosphate Mineral Dissolution Rate Parameters.

	Acid Mechanism				Neutral Mechanism	
	[a]log k	[b]E	[c]n		[a]log k	[b]E
hydroxyapatite	-4.29	250.0	0.171		-6.00	250.0
fluorapatite	-3.73	250.0	0.613		-8.00	250.0

a. Rate constant k computed from A and E, 25°C, pH = 0, mole m^{-2} s^{-1}.
b. Arrhenius activation energy E, kJ mole^{-1}.
c. Reaction order n with respect to H$^+$.

3.12 Halides

Dissolution rate data for halite (Alkattan et al., 1997a; Alkattan et al., 1997b) and fluorite (Bosbach et al., 1995; Christoffersen et al., 1988; Gardner and Nancollas, 1976; Hamza et al., 1987; Hamza and Hamdona, 1991; Zhang and Nancollas, 1990) were evaluated. Data for halite were selected from Alkattan (1997a), and the rate parameters were regressed using eqn. (11); the far from equilibrium rate constant was calculated from data at $\Omega = 0.90$ to 0.94 and the apparent rate constant. For fluorite, the rate constant at 25 °C in pure water was selected from Zhang and Nancollas (1990), where the far from equilibrium rate constant was calculated from data at $\Omega = 0.40$ and the apparent rate constant, and the activation energy was selected from Hamza and Hamdone (1991). The rate parameters for halite and fluorite are summarized in Table 37.

Table 37. Halide Mineral Dissolution Rate Parameters.

| | Acid Mechanism | | | | Neutral Mechanism | |
	[a]log k	[b]E	[c]n		[a]log k	[b]E
halite	--	--	--		-0.21	7.4
fluorite	-7.14	73.0	1.000		-13.79	73.0

a. Rate constant k computed from A and E, 25°C, pH = 0, mole m^{-2} s^{-1}.
b. Arrhenius activation energy E, kJ $mole^{-1}$.
c. Reaction order n with respect to H^+.

4. CONCLUSIONS

This work is intended as a preliminary starting point for the implementation of the kinetics of mineral dissolution and precipitation in aqueous fluids in reaction path modeling of water-rock-gas systems. The list of cited references may be as useful as, or perhaps more useful than, the rate parameters compiled herein, as the references commonly provide information to further refine rate equations that have been implemented, particularly with regard to the use of adsorption isotherms to quantify the effects of dissolved constituents upon reaction rates. The general rate equation and rate parameters were compiled specifically for the program GAMSPATH (Perkins et al., 1997), which simulates an infinitely well stirred batch reactor. For the program GAMSPATH, the rate parameters compiled provide the ability to compute, to a first approximation, the minimum length of time required for a system to equilibrate.

For most minerals, there is currently a high degree of uncertainty in experimentally determined dissolution and precipitation rates. For many minerals, variation in composition, degree of cation disorder, degree of crystallinity, as well as the frequency and distribution of crystal defects, contribute to these uncertainties. In many cases, the lack of data over a wide range of temperatures results in a large degree of uncertainty in the Arrhenius activation energy. Furthermore, the possible effects of many common dissolved species have not been quantified. It is clear that much experimental work remains to be done to determine the kinetics of mineral dissolution and precipitation under conditions that are encountered in natural systems.

REFERENCES

Aagaard P. and Helgeson H. C. (1982) Thermodynamic and kinetic constraints on reaction rates among minerals and aqueous solutions. I. Theoretical considerations. *Am. J. Sci.* 282, 237-285.

Acker J. G. and Bricker O. P. (1992) The influence of pH on biotite dissolution and alteration kinetics at low temperature. *Geochim. Cosmochim. Acta* 56, 3073-3092.

Alekseyev V. A., Medvedeva L. S., Prisyagina N. I., Meshalkin S. S., and Balabin A. I. (1997) Change in the dissolution rates of alkali feldspars as a result of secondary mineral precipitation and approach to equilibrium. *Geochim. Cosmochim. Acta* 61, 1125-1142.

Alkattan M., Oelkers E. H., Dandurand J.-L., and Schott J. (1997a) Experimental studies of halite dissolution kinetics: I. The effect of saturation state and the presence of trace metals. *Chem. Geol.* 137, 201-219.

Alkattan M., Oelkers E. H., Dandurand J.-L., and Schott J. (1997b) Experimental studies of halite dissolution kinetics: II. The effect of the presence of aqueous trace anions and $K_3Fe(CN)_6$. *Chem. Geol.* 143, 17-26.

Alkattan M., Oelkers E. H., Dandurand J.-L., and Schott J. (1998) An experimental study of calcite and limestone dissolution rates as a function of pH from -1 to 3 and temperature from 25 to 80°C. *Chem. Geol.* 151, 199-214.

Alkattan M., Oelkers E. H., Dandurand J.-L., and Schott J. (2002) An experimental study of calcite dissolution rates at acidic conditions and 25 °C in the presence of $NaPO_3$ and $MgCl_2$. *Chem. Geol.* 190, 291-302.

Altaner S. P. (1986) Comparison of rates of smectite illitization with rates of feldspar dissolution. *Clays and Clay Minerals* 34, 608-611.

Amrhein C. and Suarez D. (1988) The use of a surface complexation model to describe the kinetics of ligand-promoted dissolution of anorthite. *Geochim. Cosmochim. Acta* 52, 2785-2793.

Amrhein C. and Suarez D. L. (1992) Some factors affecting the dissolution kinetics of anorthite at 25°C. *Geochim. Cosmochim. Acta* 56, 1815-1826.

Anbeek C. (1993) The effect of natural weathering on dissolution rates. *Geochim. Cosmochim. Acta* 57, 4963-4975.

Arnórsson S. (1983) Chemical equilibria in Icelandic geothermal systems- implications for chemical geothermometry investigations. *Geothermics* 12, 119-128.

Arnórsson S., Gunnlaugsson E., and Hördur S. (1983) The chemistry of geothermal waters in Iceland. II. Mineral equilibria and independent variables controlling water compositions. *Geochim. Cosmochim. Acta* 47, 547-566.

Arvidson R. S. and Mackenzie F. T. (1999) The dolomite problem: Control of precipitation kinetics by temperature and saturation state. *Am. J. Sci.* 293, 257-288.

Awad A., Koster van Groos A. F., and Guggenheim S. (2000) Forsteritic olivine: Effect of crystallographic direction on dissolution kinetics. *Geochim. Cosmochim. Acta* 64, 1765-1772.

Bailey A. (1974) Effects of temperature on the reaction of silicates with aqueous solutions in the low temperature range. *International Symposium on Water-Rock Interaction (1st).* 1976, Praha. 375-380.

Baker P. A. and Kastner M. (1981a) Constraints on the Formation of Sedimentary Dolomite. *Science* 213, 214-216.

Baker P. A. and Kastner M. (1981b) Mechanism and kinetics of sulfate inhibition on dolomitization of calcium carbonate. *The American Association of Petroleum Geologists Bulletin* 65, 893-894.

Bales R. C. and Morgan J. J. (1985) Dissolution kinetics of chrysotile at pH 7 to 10. *Geochim. Cosmochim. Acta* 49, 2281-2288.

Barton A. F. M. and Wilde N. M. (1971) Dissolution rates of polycrystalline samples of gypsum and orthorhombic forms of calcium sulphate by the rotating disc method. *Transactions of the Faraday Society* 67, 3590-3597.

Bauer A. and Berger G. (1998) Kaolinite and smectite dissolution rate in high molar KCl solutions at 35° and 80°C. *Appl. Geochem.* 13, 905-916.

Bazin B., Brosse E., and Sommer F. (1997a) Reconstitution de la chimie des eaux de gisement en réservoir gréseux en vue d'une modélisation numérique de la diagenèse minrérale. *Bulletin de la Société géologique de France* 168, 231-242.

Bazin B., Brosse É., and Sommer F. (1997b) Chemistry of oil-field brines in relation to diagenesis of reservoirs 1. Use of mineral stability fields to reconstruct in situ water composition. Example of the Mahakam basin. *Marine and Petroleum Geology* 14, 481-495.

Bennett P. C. (1991) Quartz dissolution in organic-rich aqueous systems. *Geochim. Cosmochim. Acta* 55, 1781-1797.

Bennett P. C., Melcer M. E., Siegel D. I., and Hassett J. P. (1988) The dissolution of quartz in dilute aqueous solutions of organic acids at 25°C. *Geochim. Cosmochim. Acta* 52, 1521-1530.

Berg A. and Banwart S. A. (2000) Carbon dioxide mediated dissolution of Ca-feldspar: implications for silicate weathering. *Chem. Geol.* 163, 25-42.

Berger G., Cadore E., Schott J., and Dove P. M. (1994) Dissolution rate of quartz in lead and sodium electrolyte solutions between 25 and 300 °C: Effect of the nature of surface complexes and reaction affinity. *Geochim. Cosmochim. Acta* 58, 541-551.

Berner R. A. and Morse J. W. (1974) Dissolution kinetics of calcium carbonate in sea water IV. Theory of calcite dissolution. *Am. J. Sci.* 274, 108-134.

Bertrand C., Fritz B., and Sureau J. F. (1994) Hydrothermal experiments and thermo-kinetic modelling of water-sandstone interactions. *Chem. Geol.* 116, 189-202.

Bevan J. and Savage D. (1989) The effect of organic acids on the dissolution of K-feldspar under conditions relevant to burial diagenesis. *Mineral. Mag.* 53, 415-425.

Bildstein O., Worden R. H., and Brosse E. (2001) Assessment of anhydrite dissolution as the rate-limiting step during thermochemical sulfate reduction. *Chem. Geol.* 176, 173-189.

Bird G., Boon J., and Stone T. (1986) Silica transport during steam injection into oil sands 1. dissolution and precipitation kinetics of quartz: new results and review of existing data. *Chem. Geol.* 50, 69-80.

Blake R. E. and Walter L. M. (1996) Effects of organic acids on the dissolution of orthoclase at 80°C and pH 6. *Chem. Geol.* 132, 91-102.

Blake R. E. and Walter L. M. (1999) Kinetics of feldspar and quartz dissolution at 70-80°C and near-neutral pH: Effect of organic acids and pH. *Geochim. Cosmochim. Acta* 63, 2043-2059.

Bloom P. R. (1983) The kinetics of gibbsite dissolution in nitric acid. *Soil Sci. Soc. Am. J.* 47, 164-168.

Bloom P. R. and Erich M. S. (1987) Effect of solution composition on the rate of gibbsite dissolution in acidic solutions. *Soil Sci. Soc. Am. J.* 51, 1131-1136.

Blum A. E. and Lasaga A. C. (1986) Forsterite dissolution kinetics. *EOS* 67, 1278-1279.

Blum A. E. and Lasaga A. C. (1991) The role of surface speciation in the dissolution of albite. *Geochim. Cosmochim. Acta* 55, 2193-2201.

Blum A. E. and Stillings L. L. (1995) Feldspar dissolution kinetics. In *Chemical Weathering Rates of Silicate Minerals* (eds. A. F. White and S. L. Brantley). Mineralogical Society of America, Washington, D.C. pp. 291-351.

Blum A. E., Yund R. A., and Lasaga A. C. (1990) The effect of dislocation density on the dissolution rate of quartz. *Geochim. Cosmochim. Acta* 54, 283-297.

Bosbach D., Jordan G., and Rammensee W. (1995) Crystal growth and dissolution kinetics of gypsum and fluorite; an in situ scanning force microscope study. *Euro. J. Min.* 7, 267-276.

Brady P. V. (1992) Silica surface chemistry at elevated temperatures. *Geochim. Cosmochim. Acta* 56, 2941-2946.

Brady P. V. and Walther J. V. (1989) Controls on silicate dissolution rates in neutral and basic pH solutions at 25°C. *Geochim. Cosmochim. Acta* 53, 2823-2830.

Brady P. V. and Walther J. V. (1990) Kinetics of quartz dissolution at low temperatures. *Chem. Geol.* 82, 253-264.

Brantley S. L. and Chen Y. (1995) Chemical weathering rates of pyroxenes and amphiboles. In *Chemical Weathering Rates of Silicate Minerals* (eds. A. F. White and S. L. Brantley). Mineralogical Society of America, Washington, D.C. pp. 119-172.

Brantley S. L. and Stillings L. (1994) An integrated model for feldspar dissolution under acid conditions. *Mineral. Mag.* 58A, 117-118.

Brown C. A., Compton R. G., and Narramore C. A. (1993) The kinetics of calcite dissolution/precipitation. *J. Coll. Interface Sci.* 160, 372-379.

Bruno J. and Duro L. (2000) Reply to W. Hummel's comment on and correction to "On the influence of carbonate in mineral dissolution: 1. The thermodynamics and kinetics of hematite dissolution in bicarbonate solutions at T = 25 °C" by J. Bruno, W. Stumm, P. Wersin, and F. Brandberg, Frederick. *Geochim. Cosmochim. Acta* 64, 2173-2176.

Bruno J., Stumm W., Wersin P., and Brandberg F. (1992) On the influence of carbonate in mineral dissolution; 1, The thermodynamics and kinetics of hematite dissolution in bicarbonate solutions at T = 25 °C. *Geochim. Cosmochim. Acta* 56, 1139-1147.

Burch T. E., Nagy K. L., and Lasaga A. C. (1993) Free energy dependence of albite dissolution kinetics at 80°C and pH 8.8. *Chem. Geol.* 105, 137-162.

Busenberg E. and Clemency C. V. (1976) The dissolution kinetics of feldspars at 25°C and 1 atm CO_2 partial pressure. *Geochim. Cosmochim. Acta* 40, 41-49.

Busenberg E. and Plummer L. N. (1982) The kinetics of dissolution of dolomite in CO_2-H_2O systems at 1.5 to 65°C and 0 to 1 atm $P(CO_2)$. *Am. J. Sci.* 282, 45-78.

Busenberg E. and Plummer L. N. (1986) A comparative study of the dissolution and crystal growth of calcite and aragonite. *USGS Bull.* 1578, 139-168.

Cama J., Ganor J., Ayora C., and Lasaga A. C. (2000) Smectite dissolution kinetics at 80°C and pH 8.8. *Geochim. Cosmochim. Acta* 64, 2701-2717.

Cama J., Ganor J., and Lasaga A. C. (1994) The kinetics of smectite dissolution. *Mineral. Mag.* 58A, 140-141.

Cama J., Metz V., and Ganor J. (2002) The effect of pH and temperature on kaolinite dissolution rate under acidic conditions. *Geochim. Cosmochim. Acta* 66, 3913-3926.

Carroll S. A. and Knauss K. (2001) Experimental determination of Ca-silicate dissolution rates: A source of calcium for geologic sequestration. *DOE/NETL First National Conference on Carbon Sequestration.* May 14-17, 2001, Washington, DC.

Carroll S. A. and Walther J. V. (1990) Kaolinite dissolution at 25°, 60°, and 80°C. *Am. J. Sci.* 290, 797-810.

Carroll-Webb S. A. and Walther J. V. (1988) A surface complex reaction model for the pH-dependence of corundum and kaolinite dissolution rates. *Geochim. Cosmochim. Acta* 52, 2609-2623.

Casey W. H. and Sposito G. (1992) On the temperature dependence of mineral dissolution rates. *Geochim. Cosmochim. Acta* 56, 3825-3830.

Casey W. H., Westrich H. R., and Holdren G. R. (1991) Dissolution rates of plagioclase at pH = 2 and 3. *Am. Min.* 76, 211-217.

Cetisli H. and Gedikbey T. (1990) Dissolution kinetics of sepiolite from Eskisehir (Turkey) in hydrochloric and nitric acids. *Clay Minerals* 25, 207-215.

Chang B.-T., Pak L.-H., and Li Y.-S. (1979) Solubilities and rates of dissolution of diaspore in NaOH aqueous solutions. *Bull. Chem. Soc. Japan* 52, 1321-1326.

Chen Y. and Brantley S. (2000) Dissolution of forsteritic olivine at 65°C and 2<pH<5. *Chem. Geol.* 165, 267-281.

Chen Y. and Brantley S. L. (1997) Temperature dependence of albite dissolution rate at acid pH. *Chem. Geol.* 135, 275-290.

Chen Y. and Brantley S. L. (1998) Diopside and anthophyllite dissolution at 25° and 90°C and acid pH. *Chem. Geol.* 147, 233-248.

Chen Y., Brantley S. L., and Ilton E. S. (2000) X-ray photoelectron spectroscopic measurement of the temperature dependence of leaching of cations from the albite surface. *Chem. Geol.* 163, 115-128.

Chien S. H. (1977) Dissolution rates of phosphate rocks. *Soil Sci. Soc. Am. J.* 41, 656-657.

Chien S. H., Clayton W. R., and McClellan G. H. (1980) Kinetics of dissolution of phosphate rocks in soils. *Soil Sci. Soc. Am. J.* 44, 260-264.

Chou L., Garrels R. M., and Wollast R. (1989) Comparative study of the kinetics and mechanisms of dissolution of carbonate minerals. *Chem. Geol.* 78, 269-282.

Chou L. and Wollast R. (1984) Study of the weathering of albite at room temperature and pressure with a fluidized bed reactor. *Geochim. Cosmochim. Acta* 48, 2205-2217.

Chou L. and Wollast R. (1985) Steady-state kinetics and dissolution mechanisms of albite. *Am. J. Sci.* 285, 963-993.

Christoffersen J., Christoffersen M. R., Kibalczyc W., and Perdok W. G. (1988) Kinetics of dissolution and growth of calcium fluoride and effects of phosphate. *Acta Odontologica Scandinavica* 46, 325-336.

Christoffersen J., Christoffersen M. R., and Kjaergaard N. (1978) The kinetics of dissolution of calcium hydroxyapatite in water at constant pH. *J. Crystal Growth* 43, 501-511.

Christy A. G. and Putnis A. (1993) The kinetics of barite dissolution and precipitation in water and sodium chloride brines at 44-85 °C. *Geochim. Cosmochim. Acta* 57, 2161-2168.

Clemency C. V. and Lin F.-C. (1981) Dissolution kinetics of phlogopite. I. Open system using an ion-exchange resin. *Clays and Clay Minerals* 29, 107-112.

Dekkers M. J. and Schoonen M. A. A. (1994) An electrokinetic study of synthetic griegite and pyrrhotite. *Geochim. Cosmochim. Acta* 58, 4147-4153.

Deleuze M. and Brantley S. L. (1997) Inhibition of calcite crystal growth by Mg^{2+} at 100°C and 100 bars: Influence of growth regime. *Geochim. Cosmochim. Acta* 61, 1475-1485.

Devidal J. L., Schott J., and Dandurand J.-L. (1997) An experimental study of kaolinite dissolution and precipitation kinetics as a function of chemical affinity and solution composition at 150°C, 40 bars, and pH 2, 6.8, and 7.8. *Geochim. Cosmochim. Acta* 61, 5165-5186.

Dove P. M. (1994) The dissolution kinetics of quartz in sodium chloride solutions at 25° to 300°C. *Am. J. Sci.* 294, 665-712.

Dove P. M. (1999) The dissolution kinetics of quartz in aqueous mixed cation solutions. *Geochim. Cosmochim. Acta* 63, 3715-3727.

Dove P. M. and Crerar D. A. (1990) Kinetics of quartz dissolution in electrolyte solutions using a hydrothermal mixed flow reactor. *Geochim. Cosmochim. Acta* 54, 955-969.

Dove P. M. and Czank C. A. (1995) Crystal chemical controls on the dissolution kinetics of the isostructural sulfates; celestite, anglesite and barite. *Geochim. Cosmochim. Acta* 59, 1907-1915.

Dove P. M. and Elston S. F. (1992) Dissolution kinetics of quartz in sodium chloride solutions: Analysis of existing data and a rate model for 25°C. *Geochim. Cosmochim. Acta* 56, 4147-4156.

Dove P. M. and Nix C. J. (1997) The influence of the alkaline earth cations, magnesium, calcium, and barium on the dissolution kinetics of quartz. *Geochim. Cosmochim. Acta* 61, 3329-3340.

Fawzi M. B., Fox J. L., Dedhiya M. G., Higuchi W. I., and Hefferren J. H. (1978) A possible second site for hydroxyapatite dissolution in acidic media. *J. Coll. Interface Sci.* 67, 304-311.

Fenter P., Park C., Cheng L., Zhang Z., Krekeler M. P. S., and Sturchio N. C. (2003) Orthoclase dissolution kinetics probed by in situ X-ray reflectivity: Effects of temperature, pH, and crystal orientation. *Geochim. Cosmochim. Acta* 67, 197-211.

Fleer V. N. and Johnston R. M. (1986) A compilation of solubility and dissolution kinetics data on minerals in granitic and gabbroic systems. 170 pp.

Fox J. L., Higuchi W. I., Fawzi M. B., and Wu M.-S. (1978) A new two-site model for hydroxyapatite dissolution in acidic media. *J. Coll. Interface Sci.* 67, 312-330.

Furrer G. and Stumm W. (1986) The coordination chemistry of weathering: I. Dissolution kinetics of Delta-Al_2O_3 and BeO. .

Furrer G., Zysset M., and Schindler P. W. (1993) Weathering kinetics of montmorillonite: Investigations in batch and mixed-flow reactors. In *Geochemistry of clay-pore fluid interactions* (eds. D. A. C. Manning, P. L. Hall, and C. R. Hughes). Chapman & Hall, London, New York. pp. 243-262.

Gaines A. M. (1980) Dolomitization kinetics: Recent experimental studies. In *Concepts and Models of Dolomitization* (ed. D. H. Zenger). Society of Economic Paleontologists and Mineralogists, Tulsa. pp. 81-86.

Gallup D. L. (1998) Aluminum silicate scale formation and inhibition 2): scale solubilities and laboratory and field inhibition tests. *Geothermics* 27, 485-501.

Ganor J., Mogollón J. L., and Lasaga A. C. (1995) The effect of pH on kaolinite dissolution rates and on activation energy. *Geochim. Cosmochim. Acta* 59, 1037-1052.

Ganor J., Mogollón J. L., and Lasaga A. C. (1999) Kinetics of gibbsite dissolution under low ionic strength conditions. *Geochim. Cosmochim. Acta* 63, 1635-1651.

Gardner G. L. and Nancollas C. H. (1976) Kinetics of crystal growth and dissolution of calcium and magnesium fluourides. *Journal of Dental Research* 55, 342-352.

Gautelier M., Oelkers E. H., and Schott J. (1999) An experimental study of dolomite dissolution rates as a function of pH from -0.5 to 5 and temperature from 25 to 80°C. *Chem. Geol.* 157, 13-26.

Gautier J.-M., Oelkers E. H., and Schott J. (1994) Experimental studies of K-feldspar dissolution rates as a function of chemical affinity at 150°C and pH 9. *Geochim. Cosmochim. Acta* 58, 4549-4560.

Gautier J.-M., Oelkers E. H., and Schott J. (2001) Are quartz dissolution rates proportional to B.E.T. surface areas? *Geochim. Cosmochim. Acta* 65, 1059-1070.

Gérard F., Fritz B., Clément A., and Crovisier J.-L. (1998) General implications of aluminum speciation-dependent kinetic dissolution rate law in water-rock modelling. *Chem. Geol.* 151, 247-258.

Gibbs M. D., Smith T. N., and Verbaan B. (1997a) Kinetics of pyrite decomposition in a fluidized bed-Part 1: Removal of ambient sulphur vapour is rate-limiting. *Transactions of the Institution of Mining and Metallurgy. Section C: Mineral Processing and Extractive Metallurgy* 106, 69-73.

Gibbs M. D., Smith T. N., and Verbaan B. (1997b) Kinetics of pyrite decomposition in a fluidized bed-Part 2: Influence of transfer processes in the bed. *Transactions of the Institution of Mining and Metallurgy. Section C: Mineral Processing and Extractive Metallurgy* 106, 74-79.

Giggenbach W. F. (1980) Geothermal gas equilibria. *Geochim. Cosmochim. Acta* 44, 2021-2032.

Giggenbach W. F. (1981) Geothermal mineral equilibria. *Geochim. Cosmochim. Acta* 45, 393-410.

Grandstaff D. E. (1976) A kinetic study of the dissolution of uraninite. *Econ. Geol.* 71, 1493-1506.

Grandstaff D. E. (1986) The dissolution rate of forsteritic olivine from Hawaiian beach sand. *International Symposium on Water-Rock Interaction* Edmonton, Canada. 72-74.

Greenberg J. and Tomson M. (1992) Precipitation and dissolution kinetics and equilibria of aqeous ferrous carbonate vs temperature. *Appl. Geochem.* 7, 185-190.

Gronow J. R. (1987) The dissolution of asbestos fibres in water. *Clay Minerals* 22, 21-35.

Guidry M. W. and Mackenzie F. T. (2003) Experimental study of igneous and sedimentary apatite dissolution: Control of pH, distance from equilibrium, and temperature on dissolution rates. *Geochim. Cosmochim. Acta* 67, 2949-2963.

Gunter W. D., Wiwchar B., and Perkins E. H. (1997) Aquifer disposal of CO_2-rich greenhouse gases: Extension of the time scale of experiment for CO_2-sequestering reactions by geochemical modeling. *Mineralogy and Petrology* 59, 121-140.

Hajash A., Jr., Carpenter T. D., and Dewers T. A. (1998) Dissolution and time-dependent compaction of albite sand: experiments at 100°C and 160°C in pH buffered organic acids and distilled water. *Tectonophysics* 295, 93-115.

Hamilton J. P., Brantley S. L., Pantano C. G., Criscenti L. J., and Kubicki J. D. (2001) Dissolution of nepheline, jadeite, and albite glasses: Toward better models for aluminosilicate dissolution. *Geochim. Cosmochim. Acta* 65, 3683-3702.

Hamza S. M., Aly F. A., and El-Ries M. A. (1987) Kinetics of dissolution of alkaline earth fluorides. *Indian Journal of Chemistry* 26A, 301-303.

Hamza S. M. and Hamdona S. K. (1991) Kinetics of dissolution of calcium fluoride crystals in sodium chloride solutions: Influence of additives. *J. Phys. Chem.* 95, 3149-3152.

Hayashi H. and Yamada M. (1990) Kinetics of dissolution of noncrystalline oxides and crystalline clay minerals in a basic tiron solution. *Clays and Clay Minerals* 38, 308-314.

Helgeson H. C. (1970) Reaction rates in hydrothermal flow systems. *Econ. Geol.* 65, 299-303.

Helgeson H. C., Murhpy W. M., and Aagaard P. (1984) Thermodynamic and kinetic constraints on reaction rates among minerals and aqueous solutions. II. Rate constants, effective surface area, and the hydrolysis of feldspar. *Geochim. Cosmochim. Acta* 48, 2405-2432.

Hellman R. (1994a) The albite-water system: Part I. The kinetics of dissolution as a function of pH at 100, 200, and 300°C. *Geochim. Cosmochim. Acta* 58, 595-611.

Hellman R. (1994b) A leached layer hydrolysis model: a better way to understanding feldspar dissolution at elevated temperatures and pressures? *Mineral. Mag.* 58A, 400-401.

Hellman R. (1995) The albite-water system: Part II. The time-evolution of the stoichiometry of dissolution as a function of pH at 100, 200, and 300°C. *Geochim. Cosmochim. Acta* 59, 1669-1697.

Higgins S. R., Jordan G., and Eggleston C. M. (2002) Dissolution kinetics of magnesite in acidic solutions: A hydrothermal atomic force microscopy study assessing step kinetics and dissolution flux. *Geochim. Cosmochim. Acta* 66, 3201-3210.

Holdren G. R., Jr. and Berner R. A. (1979) Mechanism of feldspar weathering-I. Experimental studies. *Geochim. Cosmochim. Acta* 43, 1161-1171.

Holdren G. W. and Speyer P. M. (1987) Reaction rate-surface area relationships during the early stages of weathering. II. Data on eight additional feldspars. *Geochim. Cosmochim. Acta* 51, 2311-2318.

Holmes P. R. and Crundwell F. K. (2000) The kinetics of the oxidation of pyrite by ferric ions and dissolved oxygen: An electrochemical study. *Geochim. Cosmochim. Acta* 64, 263-274.

House W. A. (1981) Kinetics of crystallisation of calcite from calcium bicarbonate solutions. *Journal of the Chemical Society, Faraday Transactions 1* 77, 341-359.

Huertas F. J., Caballero E., Jiménez de Cisneros C., Huertas F., and Linares J. (2001a) Kinetics of montmorillonite dissolution in granitic solutions. *Appl. Geochem.* 16, 397-407.

Huertas F. J., Chou L., and Wollast R. (1999a) Mechanism of kaolinite dissolution at room temperature and pressure. Part II: Kinetic Study. *Geochim. Cosmochim. Acta* 63, 3261-3275.

Huertas F. J., Chou L., and Wollast R. (2001b) Kaolinite dissolution rates in batch experiments at room temperature and pressure: Reply to "On the interpretation of closed system mineral dissolution experiments," Comment by Eric H. Oelkers, Jacques Schott, and Jean-Luc Devidal. *Geochim. Cosmochim. Acta* 65, 4433-4434.

Huertas F. J., Fiore S., Huertas F., and Linares J. (1999b) Experimental study of the hydrothermal formation of kaolinite. *Chem. Geol.* 156, 171-190.

Hull A. B. and Hull J. R. (1987) Geometric modeling of dissolution kinetics; application to apatite. *Water Resources Research* 23, 707-714.

Hume L. A. and Rimstidt J. D. (1992) The biodurability of chrysotile asbestos. *Am. Min.* 77, 1125-1128.

Hummel W. (2000) Comment on "On the influence of carbonate in mineral dissolution: 1. The thermodynamics and kinetics of hematite dissolution in bicarbonate solutions at T = 25 °C" by J. Bruno, W. Stumm, P. Wersin, and F. Brandberg, Frederick. *Geochim. Cosmochim. Acta* 64, 2167-2171.

Incenhower J. P. and Dove P. M. (2000) The dissolution kinetics of amorphous silica into sodium chloride solutions: Effects of temperature and ionic strength. *Geochim. Cosmochim. Acta* 64, 4193-4203.

Inskeep W. P. and Bloom P. R. (1985) An evaluation of rate equations for calcite precipitation kinetics at pCO$_2$ less than 0.01 atm and pH greater than 8. *Geochim. Cosmochim. Acta* 49, 2165-2180.

Janzen M. P., Nicholson R. V., and Scharper J. M. (2000) Pyrrhotite reaction kinetics: Reaction rates for oxidation by oxygen, ferric iron, and for nonoxidative dissolution. *Geochim. Cosmochim. Acta* 64, 1511-1522.

Jensen D. L., Boddum J. K., Tjell J. C., and Christensen T. H. (2002) The solubility of rhodochrosite MnCO$_3$ and siderite FeCO$_3$ in anaerobic aquatic environments. *Appl. Geochem.* 17, 503-511.

Jeschke A. A. and Dreybrodt W. (2002a) Dissolution rates of minerals and their relation to surface morphology. *Geochim. Cosmochim. Acta* 66, 3055-3062.

Jeschke A. A. and Dreybrodt W. (2002b) Pitfalls in the determination of empirical dissolution rate equations of minerals from experimental data and a way out: an iterative procedure to find valid rate equations, applied to Ca-carbonates and -sulphates. *Chem. Geol.* 192, 183-194.

Jeschke A. A., Vosbeck K., and Dreybrodt W. (2001) Surface controlled dissolution rates of gypsum in aqueous solutions exhibit nonlinear dissolution kinetics. *Geochim. Cosmochim. Acta* 65, 27-34.

Jiménez-López C., Caballero E., Huertas F. J., and Romanek C. S. (2001) Chemical, mineralogical, and isotope behavior, and phase transformation during the precipitation of calcium carbonate minerals from intermediate ionic solutions at 25°CC. *Geochim. Cosmochim. Acta* 65, 3219-3231.

Johnson J. W., Nitao J. J., Steefel C. I., and Knauss K. G. (2001) Reactive transport modeling of geologic CO$_2$ sequestration in saline aquifers: the influence of intra-aquifer shales and the relative effectiveness of structural, solubility, and mineral trapping during prograde and retrograde sequestration. *First National Conference on Carbon Sequestration.* May 14-17, 2001, Washington, D.C. 60 pp.

Jonckbloedt R. C. L. (1998) Olivine dissolution in sulphuric acid at elevated temperatures-- implications for the olivine process, an alternative waste acid neutralizing process. *Journal of Geochemical Exploration* 62, 337-346.

Jordan G., Higgins S. R., Eggleston C. M., Knauss K. G., and Schmahl W. W. (2001) Dissolution kinetics of magnesite in aqueous solution, a hydrothermal atomic force microscopy study: Step orientation and kink dynamics. *Geochim. Cosmochim. Acta* 65, 4257-4266.

Jordan G. and Rammensee W. (1996) Dissolution rates and activation energy of brucite (001): A new method based on the microtopography of crystal surfaces. *Geochim. Cosmochim. Acta* 60, 5055-5062.

Jordan G. and Rammensee W. (1998) Dissolution rates of calcite (1014) obtained by scanning force microscopy: Microtopography-based dissolution kinetics on surfaces with anisotropic step velocities. *Geochim. Cosmochim. Acta* 62, 941-947.

Kalinowski B. E., Faith-Ell C., and Schweda P. (1998) Dissolution kinetics and alteration of epidote in acidic solutions at 25°C. *Chem. Geol.* 151, 181-197.

Kalinowski B. E. and Schweda P. (1996) Kinetics of muscovite, phlogopite, and biotite dissolution and alteration at pH 1-4, room temperature. *Geochim. Cosmochim. Acta* 60, 367-385.

Kamei G. and Ohmoto H. (2000) The kinetics of reactions between pyrite and O_2-bearing water revealed from in situ monitoring of DO, Eh and pH in a closed system. *Geochim. Cosmochim. Acta* 64, 2585-2601.

Katz A. and Matthews A. (1977) The dolomitization of $CaCO_3$: An experimental study at 252-295°C. *Geochim. Cosmochim. Acta* 41, 297-308.

Kitahara. (1960) The solubility equilibrium and the rate of solution of quartz in water at high temperatures and pressures. *Reviews in Physical Chemistry, Japan* 30, 122-130.

Kline W. E. and Fogler H. S. (1981) Dissolution Kinetics: Catalysis by Salts. *J. Coll. Interface Sci.* 82, 103-115.

Knauss K. G. and Copenhaver S. A. (1995) The effect of malonate on the dissolution kinetics of albite, quartz, and microcline as a function of pH at 70°C. *Appl. Geochem.* 10, 17-33.

Knauss K. G., Nguyen S. N., and Weed H. C. (1993) Diopside dissolution kinetics as a function of pH, CO_2 temperature, and time. *Geochim. Cosmochim. Acta* 57, 285-294.

Knauss K. G. and Wolery T. J. (1986) Dependence of albite dissolution kinetics on pH and time at 25° and 70°C. *Geochim. Cosmochim. Acta* 50, 2481-2497.

Knauss K. G. and Wolery T. J. (1988) The dissolution kinetics of quartz as a function of pH and time at 70°C. *Geochim. Cosmochim. Acta* 52, 43-53.

Knauss K. G. and Wolery T. J. (1989) Muscovite dissolution kinetics as a function of pH and time at 70°C. *Geochim. Cosmochim. Acta* 53, 1493-1501.

Kornicker W. A., Presta P. A., Paige C. R., Johnson D. M., Hileman O. E., Jr., and Snodgrass W. J. (1991) The aqueous dissolution kinetics of the barium/lead sulfate solid solution series at 25 and 60 °C. *Geochim. Cosmochim. Acta* 55, 3531-3541.

Kuwahara Y. and Aoke Y. (1999) Dissolution kinetics of phlogopite under acid conditions. *Clay Science* 11, 31-45.

Lagache M. (1965) Contribution à l'étude de l'altération des feldspaths, dans l'eau, entre 100 et 200°C, sous diverses pressions de CO_2, et application à la synthèse des minéraux argileux (Contribution to the study of feldspar alteration in water, between 100 and 200°C, under varying CO_2 pressures, and its application to the synthesis of clay minerals). *Bulletin de la Societe Francaise de Mineralogie et de Cristallographie* 88, 223-253.

Lagache M. (1976) New data on the kinetics of the dissolution of alkali feldspars at 200°C in CO_2 charged water. *Geochim. Cosmochim. Acta* 40, 157-161.

Lasaga A. C. (1984) Chemical kinetics of water-rock interactions. *Journal of Geophysical Research B* 89, B6, 4009-4025.

Lasaga A. C. (1995) Fundamental approaches to describing mineral dissolution and precipitation rates. In *Reviews in Mineralogy Volume 31: Chemical Weathering Rates of Silicate*

Minerals (eds. A. F. White and S. L. Brantley). Mineralogical Society of America, Washington, D.C. pp. 23-86.

Lasaga A. C. (1998) *Kinetic Theory In the Earth Sciences*. Princeton University Press, Princeton.

Lasaga A. C., Soler J. M., Ganor J., Burch T. E., and Nagy K. L. (1994) Chemical weathering rate laws and global geochemical cycles. *Geochim. Cosmochim. Acta* 58, 2361-2386.

Lebrón I. and Suárez D. L. (1996) Calcite nucleation and precipitation kinetics as affected by dissolved organic matter at 25°C and pH > 7.5. *Geochim. Cosmochim. Acta* 60, 2765-2776.

Lebrón I. and Suárez D. L. (1998) Kinetics and mechanisms of precipitation of calcite as affected by P_{CO2} and organic ligands at 25°C. *Geochim. Cosmochim. Acta* 62, 405-416.

Lengke M. F. and Tempel R. N. (2001) Kinetic rates of amorphous As_2S_3 oxidation at 25 to 40°C and initial pH of 7.3 to 9.4. *Geochim. Cosmochim. Acta* 65, 2241-2255.

Lengke M. F. and Tempel R. N. (2002) Reaction rates of natural orpiment at 25 to 40°C and pH 6.8 to 8.2 and comparison with amorphous As_2S_3 oxidation. *Geochim. Cosmochim. Acta* 66, 3281-3291.

Lengke M. F. and Tempel R. N. (2003) Natural realgar and amorphous AsS oxidation kinetics. *Geochim. Cosmochim. Acta* 67, 859-871.

Lennie A. R. and Vaughan D. J. (1992) Kinetics of the marcasite-pyrite transformation: An infrared spectroscopic study. *Am. Min.* 77, 1166-1171.

Lin F.-C. and Clemency C. (1981a) The kinetics of dissolution of muscovites at 25°C and 1 atm CO_2 partial pressure. *Geochim. Cosmochim. Acta* 45, 571-576.

Lin F.-C. and Clemency C. V. (1981b) The dissolution kinetics of brucite, antigorite, talc, and phlogopite at room temperature and pressure. *Am. Min.* 66, 801-806.

Luce R. W., Bartlett R. W., and Parks G. A. (1972) Dissolution kinetics of magnesium silicates. *Geochim. Cosmochim. Acta* 36, 35-50.

Lüttge A., Bolton E. W., and Lasaga A. C. (1999) An interferometric study of the dissolution kinetics of anorthite: the role of reactive surface area. *Am. J. Sci.* 299, 652-678.

Lüttge A., Winkler U., and Lasaga A. C. (2003) Interferometric study of the dolomite dissolution: A new conceptual model for mineral dissolution. *Geochim. Cosmochim. Acta* 67, 1099-1116.

MacInnis I. N. and Brantley S. L. (1992) The role of dislocations and surface morphology in calcite dissolution. *Geochim. Cosmochim. Acta* 56, 1113-1126.

Maldonado C. F. E., Giroir G., Dandurand J. L., and Schott J. (1992) The dissolution of calcite in seawater from 40° to 90°C at atmospheric pressure and 35 $^o/_{oo}$ salinity. *Chem. Geol.* 97, 113-123.

Malmstrom M. and Banwart S. (1997) Biotite dissolution at 25°C: The pH dependence of dissolution rate and stoichiometry. *Geochim. Cosmochim. Acta* 61, 277-2799.

Manley E. P. and Evans L. J. (1986) Dissolution of feldspars by low molecular-weight aliphatic and aromatic acids. *Soil Science* 141, 106-112.

McKibben M. A. and Barnes H. L. (1986) Oxidation of pyrite in low temperature acidic solutions: Rate laws and surface textures. *Geochim. Cosmochim. Acta* 50, 1509-1520.

Metz V. and Ganor J. (2001) Stirring effect on kaolinite dissolution rate. *Geochim. Cosmochim. Acta* 65, 3475-3490.

Mogollón J. L., Ganor J., Soler J. M., and Lasaga A. C. (1996) Column experiments and the full dissolution rate law of gibbsite. *Am. J. Sci.* 296, 729-765.

Mogollón J. L., Pérez-Diaz A., and Lo Monaco S. (2000) The effects of ion identity and ionic strength on the dissolution rate of a bauxitic gibbsite. *Geochim. Cosmochim. Acta* 64, 781-795.

Morse J. W. (1978) Dissolution kinetics of calcium carbonate in sea water: VI. The near-equilibrium dissolution kinetics of calcium carbonate-rich deep sea sediments. *Am. J. Sci.* 278, 344-353.

Moses C. O. and Herman J. S. (1991) Pyrite oxidation at circumneutral pH. *Geochim. Cosmochim. Acta* 55, 471-482.

Moses C. O., Nordstrom D. K., Herman J. S., and Mills A. L. (1987) Aqueous pyrite oxidation by dissolved oxygen and by ferric iron. *Geochim. Cosmochim. Acta* 51, 1561-1571.

Mucci A. (1986) Growth kinetics and composition of magnesian calcite overgrowths precipitated from seawater: Quantitative influence of orthophosphate ions. *Geochim. Cosmochim. Acta* 50, 2255-2265.

Mucci A. and Morse J. W. (1983) The incorporation of Mg^{2+} and Sr^{2+} into calcite overgrowths; influences of growth rate and solution composition. *Geochim. Cosmochim. Acta* 47, 217-233.

Murakami T., Kogure T., Kadohara H., and Ohnuki T. (1998) Formation of secondary minerals and its effect on anorthite dissolution. *Am. Min.* 83, 1209-1219.

Murphy W. M. and Helgeson H. C. (1987) Thermodynamic and kinetic constraints on reaction rates among minerals and aqueous solutions. III. Activated complexes and the pH-dependence of the rates of feldspar, pyroxene, wollastonite, and olivine hydrolysis. *Geochim. Cosmochim. Acta* 51, 3137-3153.

Murphy W. M. and Helgeson H. C. (1989) Thermodynamic and kinetic constraints on reaction rates among minerals and aqueous solutions; IV, Retrieval of rate constants and activation parameters for the hydrolysis of pyroxene, wollastonite, olivine, andalusite, quartz, and nepheline. *Am. J. Sci.* 289, 17-101.

Nagy K. L. (1995) Dissolution and precipitation kinetics of sheet silicates. In *Chemical Weathering Rates of Silicate Minerals* (eds. A. F. White and S. L. Brantley). Mineralogical Society of America, Washington, D.C. pp. 173-233.

Nagy K. L., Blum A. E., and Lasaga A. C. (1991) Dissolution and precipitation kinetics of kaolinite at 80°C and pH 3: The dependence on the solution saturation state. *Am. J. Sci.* 291, 649-686.

Nagy K. L. and Lasaga A. C. (1990) The effect of deviation from equilibrium on the kinetics of dissolution of kaolinite and gibbsite. *Chem. Geol.* 84, 283-285.

Nagy K. L. and Lasaga A. C. (1992) Dissolution and precipitation kinetics of gibbsite at 80°C and pH 3: The dependence on solution saturation state. *Geochim. Cosmochim. Acta* 56, 3093-3111.

Nagy K. L. and Lasaga A. C. (1993) Simultaneous precipitation kinetics of kaolinite and gibbsite at 80°C and pH 3. *Geochim. Cosmochim. Acta* 57, 4329-4335.

Nicholson R. V., Gillham R. W., and Reardon E. J. (1988) Pyrite oxidation in carbonate-buffered solution: 1. Experimental kinetics. *Geochim. Cosmochim. Acta* 52, 1077-1085.

Nicholson R. V., Gillham R. W., and Reardon E. J. (1990) Pyrite oxidation in carbonate-buffered solution: 2. Rate control by oxide coatings. *Geochim. Cosmochim. Acta* 54, 395-402.

Nordeng S. H. and Sibley D. F. (1994) Dolomite stoichiometry and Ostwald's step rule. *Geochim. Cosmochim. Acta* 58, 191-196.

Normand C., Williams-Jones A. E., Martin R. F., and Vali H. (2002) Hydrothermal alteration of olivine in a flow-through autoclave: Nucleation and growth of serpentine phases. *Am. Min.* 87, 1699-1709.

Novák I. and Cícel B. (1978) Dissolution of smectites in hydrochloric acid: II. Dissolution rate as a function of crystallochemical composition. *Clays and Clay Minerals* 26, 341-344.

Oelkers E. H. (2001a) An experimental study of forsterite dissolution rates as a function of temperature and aqueous Mg and Si concentrations. *Chemical Geology* 175, 485-494.

Oelkers E. H. (2001b) General kinetic description of multioxide silicate mineral and glass dissolution. *Geochim. Cosmochim. Acta* 65, 3703-3719.

Oelkers E. H. and Gislason S. (2001) The mechanism, rates, and consequences of basaltic glass dissolution: I. An experimental study of the dissolution rates of basaltic glass as a function of aqueous Al, Si and oxalic acid concentration at 25°C and pH 3 and 11. *Geochim. Cosmochim. Acta* 65, 3671-3681.

Oelkers E. H. and Schott J. (1995) Experimental study of anorthite dissolution and the relative mechanism of feldspar hydrolysis. *Geochim. Cosmochim. Acta* 59, 5039-5053.

Oelkers E. H. and Schott J. (1999) Experimental study of kyanite dissolution rates as a function of chemical affinity and solution composition. *Geochim. Cosmochim. Acta* 63, 785-797.

Oelkers E. H., Schott J., and Devidal J.-L. (1994) The effect of aluminum, pH, and chemical affinity on the rates of aluminosilicate dissolution reactions. *Geochim. Cosmochim. Acta* 58, 2011-2024.

Oelkers E. H., Schott J., and Jean-Luc D. (2001) On the interpretation of closed system mineral dissolution experiments: Comment on "Mechanism of kaolinite dissolution at room temperature and pressure Part II: Kinetic Study" by Huertas et al. (1999). *Geochim. Cosmochim. Acta* 65, 4429-4432.

Oxburgh R., Drever J. I., and Sun Y.-T. (1994) Mechanism of plagioclase dissolution in acid solution at 25°C. *Geochim. Cosmochim. Acta* 58, 661-669.

Packter A. and Dhillon H. S. (1974) Studies on recrystallized aluminium hydroxide precipitates: Kinetics and mechanism of dissolution by sodium hydroxide solutions. *Colloid Polym. Sci.* 252, 249-256.

Palandri J. L. and Reed M. H. (2001) Reconstruction of in situ composition of sedimentary formation waters. *Geochim. Cosmochim. Acta* 65, 1741-1767.

Pang Z. and Reed M. H. (1998) Theoretical chemical thermometry on geothermal waters: Problems and methods. *Geochim. Cosmochim. Acta* 62, 1082-1091.

Perkins E. H., Gunter W. D., Nesbitt H. W., and St-Arnaud L. C. (1997) Critical review of classes of geochemical computer models adaptable for prediction of acidic drainage from mine waste rock. In *Proceedings: Fourth international conference on acid rock drainage* (ed. H. W. Perkins). pp. 587-601.

Petrie L. M. (1995) Molecular interpretation for SO_2 dissolution kinetics of pyrolusite, manganite, and hematite. *Geochim. Cosmochim. Acta* 10, 253-267.

Petrovich R. (1981a) Kinetics of dissolution of mechanically comminuted rock-forming oxides and silicates; II, Deformation and dissolution of oxides and silicates in the laboratory and at the Earth's surface. *Geochim. Cosmochim. Acta* 45, 1675-1686.

Petrovich R. (1981b) Kinetics of dissolution of mechanically comminuted rock-forming oxides and silicates-I. Deformation and dissolution of quartz under laboratory conditions. *Geochim. Cosmochim. Acta* 45, 1665-1674.

Plummer L. N. and Wigley T. M. L. (1976) The dissolution of calcite in CO_2-saturated solutions at 25°C and 1 atmosphere total pressure. *Geochim. Cosmochim. Acta* 40, 191-202.

Plummer L. N., Wigley T. M. L., and Parkhurst D. L. (1978) The kinetics of calcite dissolution in CO_2-water systems at 5° to 60°C and 0.0 to 1.0 atm CO_2. *Am. J. Sci.* 278, 179-216.

Plummer L. N., Wigley T. M. L., and Parkhurst D. L. (1979) Critical review of the kinetics of calcite dissolution and precipitation. In *Chemical Modeling in Aqueous Systems; Speciation, Sorption, Solubility and Kinetics* (ed. E. A. Jenne). American Chemical Society, Washington, D.C. pp. 537-573.

Pokrovsky O. S. and Schott J. (1999) Processes at the magnesium-bearing carbonates/solution interface. II. Kinetics and mechanism of magnesite dissolution. *Geochim. Cosmochim. Acta* 63, 881-897.

Pokrovsky O. S. and Schott J. (2000a) Forsterite surface composition in aqueous solutions: A combined potentiometric, electrokinetic, and spectroscopic approach. *Geochim. Cosmochim. Acta* 64, 3299-3312.

Pokrovsky O. S. and Schott J. (2000b) Kinetics and mechanism of forsterite dissolution at 25°C and pH from 1 to 12. *Geochim. Cosmochim. Acta* 64, 3313-3325.

Polzer W. L. and Hem J. D. (1965) The dissolution of kaolinite. *J. Geophys. Res.* 70, 6233-6240.

Rafal'skiy R. P. and Prisyagina N. I. (1991) Reaction of andesine with hot aqueous solutions. *Geochemistry International* 28, 72-81.

Rafal'skiy R. P., Prisyagina N. I., and Kondrushin I. B. (1990) Reaction of microcline-perthite with aqueous solutions at 150 and 250°C. *Geochemistry International* 27, 56-66.

Raines M. A. and Dewers T. A. (1997) Mixed transport/reaction control of gypsum dissolution kinetics in aqueous solutions and initiation of gypsum karst. *Chem. Geol.* 140, 29-48.

Reddy M. M. (1986) Effect of magnesium ions on calcium carbonate nucleation and crystal growth in dilute solutions at 25°C. *USGS Bull.* 1578, 169-182.

Reddy M. M. and Gaillard W. D. (1981) Kinetics of calcium carbonate (calcite)-seeded crystallization: Influence of solid/solution ratio on the reaction rate constant. *J. Coll. Interface Sci.* 80, 171-178.

Reddy M. M., Plummer L. N., and Busenberg E. (1981) Crystal growth of calcite from calcium bicarbonate solutions at constant PCO_2 and 25°C: a test of a calcite dissolution model. *Geochim. Cosmochim. Acta* 45, 1281-1289.

Reed M. H. (1982) Calculation of multicomponent chemical equilibria and reaction processes in systems involving minerals, gases and an aqueous phase. *Geochim. Cosmochim. Acta* 46, 513-528.

Reed M. H. (1997) Hydrothermal alteration and its relationship to ore field composition. In *Geochemistry of hydrothermal ore deposits* (ed. H. L. Barnes). John Wiley & Sons, New York. pp. 303-366.

Reed M. H. (1998) Calculation of simultaneous chemical equilibria in aqueous-mineral-gas systems and its application to modeling hydrothermal processes. In *Techniques in Hydrothermal Ore Deposits Geology* (eds. J. Richards and P. Larson). Economic Geology. pp. 109-124.

Reed M. H. and Spycher N. F. (1984) Calculation of pH and mineral equilibria in hydrothermal waters with application to geothermometry and studies of boiling and dilution. *Geochim. Cosmochim. Acta* 48, 1479-1492.

Rickard D. (1997) Kinetics of pyrite formation by the H_2S oxidation of iron (II) monosulfide in aqueous solutions between 25 and 125°C: The rate equation. *Geochim. Cosmochim. Acta* 61, 115-134.

Rickard D. and Luther G. W., III. (1997) Kinetics of pyrite formation by the H_2S oxidation of iron (II) monosulfide in aqueous solutions between 25 and 125°C: The mechanism. *Geochim. Cosmochim. Acta* 61, 135-147.

Rickard D. T. (1975) Kinetics and mechanism of pyrite formation at low temperatures. *Am. J. Sci.* 275, 636-652.

Rimstidt J. D. and Barnes H. L. (1980) The kinetics of silica-water reactions. *Geochim. Cosmochim. Acta* 44, 1683-1699.

Rimstidt J. D. and Dove P. M. (1986) Mineral/solution reaction rates in a mixed flow reactor; wollastonite hydrolysis. *Geochim. Cosmochim. Acta* 50, 2509-2516.

Rimstidt J. D. and Vaughan D. J. (2003) Pyrite oxidation: A state-of-the-art assessment of the reaction mechanism. *Geochim. Cosmochim. Acta* 67, 873-880.

Robie R. A., Hemingway B. S., and Wilson W. H. (1976) The heat capacities of calorimetry conference copper and of muscovite $KAl_2(AlSi_3)O_{10}(OH)_2$, pyrophyllite $Al_2Si_4O_{10}(OH)_2$, and illite $K_3(Al_7Mg)(Si_{14}AL_2)O_{40}(OH)_8$ between 15 and 375K and their standard entropies at 298.15 K. *Journal of Research of the U. S. Geological Survey* 4, 631-644.

Rose N. M. (1991) Dissolution rates of prehnite, epidote, and albite. *Geochim. Cosmochim. Acta* 55, 3273-3286.

Rosso J. J. and Rimstidt J. D. (2000) A high resolution study of forsterite dissolution rates. *Geochim. Cosmochim. Acta* 64, 797-811.

Ruan H. D. and Gilkes R. J. (1995) Acid dissolution of synthetic aluminous goethite before and after transformation to hematite by heating. *Clay Minerals* 30, 55-65.

Schoonen M. A. A. and Barnes H. L. (1991a) Mechanisms of pyrite and marcasite formation from solution: III. Hydrothermal processes. *Geochim. Cosmochim. Acta* 55, 3491-3504.

Schoonen M. A. A. and Barnes H. L. (1991b) Reactions forming pyrite and marcasite from solution: I. Nucleation of FeS_2 below 100°C. *Geochim. Cosmochim. Acta* 55, 1495-1504.

Schoonen M. A. A. and Barnes H. L. (1991c) Reactions forming pyrite and marcasite from solution: II. Via FeS precursors below 100°C. *Geochim. Cosmochim. Acta* 55, 1505-1514.

Schoonen M. A. A., Xu Y., and Strongin D. R. (1998) An introduction to geocatalysis. *Journal of Geochemical Exploration* 62, 201-215.

Schott J. and Berner R. A. (1985) Dissolution mechanisms of pyroxenes and olivines during weathering. In *The Chemistry of Weathering* (ed. J. I. Drever). Kluwer Academic Publishers, Hingham, MA.

Schott J., Berner R. A., and Sjöberg L. (1981) Mechanism of pyroxene and amphibole weathering--I. Experimental studies of iron-free minerals. *Geochim. Cosmochim. Acta* 45, 2123-2135.

Schott J., Brantley S. L., Crerar D. A., Guy C., Borcsik M., and Willaime C. (1989) Dissolution kinetics of strained calcite. *Geochim. Cosmochim. Acta* 53, 373-382.

Schwartzentruber J., Fürst W., and Renon H. (1987) Dissolution of quartz into dilute alkaline solutions at 90°C: A kinetic Study. *Geochim. Cosmochim. Acta* 51, 1867-1874.

Scotford R. F. and Glastonbury J. R. (1972a) The effect of concentration on the rates of dissolution of gibbsite and boehmite. *The Canadian Journal of Chemical Engineering* 50, 754-758.

Scotford R. F. and Glastonbury J. R. (1972b) The effect of temperature on the rates of dissolution of gibbsite and boehmite. *The Canadian Journal of Chemical Engineering* 49, 611-616.

Shiraki R. and Brantley S. L. (1995) Kinetics of near-equilibrium calcite precipitation at 100°C: An evaluation of elementary reaction-based and affinity-base rate laws. *Geochim. Cosmochim. Acta* 58, 1457-1471.

Sibley D. F., Dedoes R. E., and Bartlett T. R. (1987) Kinetics of dolomitization. *Geology* 15, 1112-1114.

Siebert H., Youdelis W. V., Leja J., and Lilge E. O. (1963) The kinetics of the dissolution of crystalline quartz in water at high temperatures and pressures. *Unit Processes in Hydrometallurgy: Metall. Soc AIME conf. 24*, pp. 284-299.

Siegel D. I. and Pfannkuch H. O. (1984) Silicate mineral dissolution at pH 4 and near standard temperature and pressure. *Geochim. Cosmochim. Acta* 48, 197-201.

Sjöberg E. L. (1976) A fundamental equation for calcite dissolution kinetics. *Geochim. Cosmochim. Acta* 40, 441-447.

Sjöberg E. L. and Rickard D. T. (1983) The influence of experimental design on the rate of calcite dissolution. *Geochim. Cosmochim. Acta* 47, 2281-2285.

Sjöberg E. L. and Rickard D. T. (1984a) Calcite dissolution kinetics: Surface speciation and the origin of the variable pH dependence. *Chem. Geol.* 42, 119-136.

Sjöberg E. L. and Rickard D. T. (1984b) Temperature dependence of calcite dissolution kinetics between 1 and 62°C at pH 2.7 to 8.4 in aqueous solutions. *Geochim. Cosmochim. Acta* 48, 185-493.

Sjöberg E. L. and Rickard D. T. (1985) The effect of added dissolved calcium on calcite dissolution kinetics in aqueous solutions at 25°C. *Chem. Geol.* 49, 405-413.

Soong C. (1993) Hydrothermal kinetics of kaolinite-water interaction at pH 4.2 and 7.3, 130°C to 230°C. Ph.D. Dissertation, Pennsylvania State University. 107 pp.

Soong C. and Barnes H. L. (1991) Kinetics of kaolinite dissolution and precipitation under hydrothermal conditions. *EOS,* 72, 308.

Steefel C. I. and Lasaga A. C. (1992) Putting transport into water-rock interaction models. *Geology* 20, 680-684.

Steefel C. I. and Van Cappellen P. (1990) A new kinetic approach to modeling water-rock interaction: The role of nucleation, precursors, and Ostwald ripening. *Geochim. Cosmochim. Acta* 54, 2657-2677.

Stillings L. L. and Brantley S. L. (1995) Feldspar dissolution at 25 degrees C and pH 3; reaction stoichiometry and the effect of cations. *Geochim. Cosmochim. Acta* 59, 1483-1496.

Stillings L. L., Drever J. I., Brantley S. L., Sun Y., and Oxburgh R. (1996) Rates of feldspar dissolution at pH 3-7 with 0-8mM oxalic acid. *Chem. Geol.* 132, 79-89.

Sutheimer S. H., Maurice P. A., and Zhou Q. (1999) Dissolution of well and poorly crystallized kaolinites: Al speciation and effects of surface characteristics. *Am. Min.* 84, 620-628.

Sverdrup H. (1990) *The Kinetics of Base Cation Release Due to Chemical Weathering.* Lund University Press, Lund, Sweden.

Swoboda-Colberg N. G. and Drever J. I. (1993) Mineral dissolution rates in plot-scale field and laboratory experiments. *Chem. Geol.* 105, 51-69.

Talman S. J. and Nesbitt H. W. (1988) Dissolution of populations of ultrafine grains with applications to the feldspars. *Geochim. Cosmochim. Acta* 52, 1467-1471.

Talman S. J., Wiwchar B., and Gunter W. D. (1990) Dissolution kinetics of calcite in the H_2O-CO_2 system along the steam saturation curve to 210°C. In *Fluid-Mineral Interactions: A Tribute to H. P. Eugster* (eds. R. J. Spenser and I.-M. Chou). Lancaster Press, Inc, San Antonio, Texas. pp. 41-55.

Taylor A. S., Blum J. D., and Lasaga A. C. (2000a) The dependence of labradorite dissolution and Sr isotope release rates on solution saturation state. *Geochim. Cosmochim. Acta* 64, 2389-2400.

Taylor A. S., Blum J. D., Lasaga A. C., and MacInnis I. C. (2000b) The kinetics of dissolution and Sr release during biotite and phlogopite weathering. *Geochim. Cosmochim. Acta* 64, 1191-1208.

Teng H. H., Dove P. M., and De Yoreo J. J. (2000) Kinetics of calcite growth: Surface processes and relationships to macroscopic rate laws. *Geochim. Cosmochim. Acta* 64, 2255-2266.

Teng H. H., Fenter P., Cheng L., and Sturchio N. C. (2001) Resolving orthoclase dissolution processes with atomic force microscopy and X-ray reflectivity. *Geochim. Cosmochim. Acta* 65, 3459-3474.

Tester J. W., Worley W. G., Robinson B. A., Grigsby C. O., and Feerer J. L. (1994) Correlating quartz dissolution kinetics in pure water from 25 to 625°C. *Geochim. Cosmochim. Acta* 58, 2407-2420.

Thomas J. E., Skinner W. M., and Smart R. S. C. (2001) A mechanism to explain sudden changes in rates and products for pyrrhotite dissolution in acid solution. *Geochim. Cosmochim. Acta* 65, 1-12.

Thomassin J. H., Goni J., Baillif P., Touray J. C., and Jaurand M. C. (1977) An XPS study of the dissolution kinetics of chrysotile in 0.1 N oxalic acid at different temperatures. *Phys. Chem. Minerals* 1, 385-398.

Tole M. P., Ármannsson H., Pang Z.-H., and Arnórsson S. (1993) Fluid/mineral equilibrium calculations for geothermal fluids and chemical geothermometry. *Geothermics* 22, 17-37.

Tole M. P., Lasaga A. C., Pantano C., and White W. B. (1986) The kinetics of dissolution of nepheline ($NaAlSiO_4$). *Geochim. Cosmochim. Acta* 50, 379-392.

Trotignon L. and Turpault M.-P. (1992) The dissolution kinetics of biotite in dilute HNO_3. In *Water-Rock Interaction: Proceedings of the 7th International Symposium on Water-Rock Interaction. Volume 1: Low Temperature Environments* (eds. Y. K. Kharaka and A. S. Maest). A.A. Balkema, Rotterdam. pp. 123-125.

Tsuzuki Y. and Suzuki K. (1980) Experimental study of the alteration process of labradorite in acid hydrothermal solutions. *Geochim. Cosmochim. Acta* 44, 673-683.

Tuncay K., Puckett J., Al-Shaeib Z., and Ortoleva P. (2002) Pits, outgrowths, and inclusions as coated grain kinetic instabilities. *Geochim. Cosmochim. Acta* 66, 3901-3912.

Utsunomiya S., Murkami T., Kadohara H., and Tsukimura K. (1999) The effect of partial pressure of carbon dioxide on anorthite dissolution. *Mineralogical Journal* 21, 1-8.

Valsami-Jones E., Ragnarsdottir K. V., Putnis A., Bosbach D., Kemp A. J., and Cressey G. (1998) The dissolution of apatite in the presence of aqueous metal cations at pH 2-7. *Chem. Geol.* 151, 215-233.

Van Herk J., Pietersen H. S., and Schuiling R. D. (1989) Neutralization of industrial waste acids with olivine - The dissolution of forsteritic olivine at 40-70°C. *Chem. Geol.* 76, 341-352.

Van Lier J. A., De Bruyn P. L., and G. O. J. T. (1960) The solubility of quartz. *J. Phys. Chem.* 64, 1675-1682.

Weill D. F. and Fyfe W. S. (1964) The solubility of quartz in the range 1000-4000 bars and 400-500 °C. *Geochim. Cosmochim. Acta* 28, 1243-1255.

Weisener C. G., Smart R. S. C., and Gerson A. R. (2003) Kinetics and mechanisms of the leaching of low Fe sphalerite. *Geochim. Cosmochim. Acta* 67, 823-830.

Weissbart E. J. and Rimstidt J. D. (2000) Wollastonite: Incongruent dissolution and leached layer formation. *Geochim. Cosmochim. Acta* 64, 4007-4016.

Welch S. A. and Ullman W. J. (1992) Dissolution of feldspars in oxalic acid solutions. In *Water-Rock Interaction: Proceedings of the 7th International Symposium on Water-Rock Interaction. Volume 1: Low Temperature Environments* (eds. Y. K. Kharaka and A. S. Maest). A.A. Balkema, Rotterdam. pp. 127-130.

Welch S. A. and Ullman W. J. (1993) The effect of organic acids on plagioclase dissolution rates and stoichiometry. *Geochim. Cosmochim. Acta* 57, 2725-2736.

Welch S. A. and Ullman W. J. (1996) Feldspar dissolution in acidic and organic solutions: Compositional and pH dependence of dissolution rate. *Geochim. Cosmochim. Acta* 60, 2939-2948.

Welch S. A. and Ullman W. J. (2000) The temperature dependence of bytownite feldspar dissolution in neutral aqueous solutions of inorganic and organic ligands at low temperature (5-35°C). *Chem. Geol.* 167, 337-354.

Westrich H. R., Cygan R. T., Casey W. H., Zemitis C., and Arnold G. W. (1993) The dissolution kinetics of mixed-cation orthosilicate minerals. *Am. J. Sci.* 293, 869-893.

White A. F., Peterson M. L., and Hochella M. F., Jr. (1994) Electrochemistry and dissolution kinetics of magnetite and ilmenite. *Geochim. Cosmochim. Acta* 58, 1859-1875.

Wieland E. and Stumm W. (1992) Dissolution kinetics of kaolinite in acidic solutions at 25°C. *Geochim. Cosmochim. Acta* 56, 3339-3355.

Wieland E., Wehrli B., and Stumm W. (1988) The coordination chemistry of weathering: III. A generalization on the dissolution rates of minerals. *Geochim. Cosmochim. Acta* 52, 1969-1981.

Wiersma C. L. and Rimstidt J. D. (1984) Rates of reaction of pyrite and marcasite with ferric iron at pH 2. *Geochim. Cosmochim. Acta* 48, 85-92.

Williamson M. A. and Rimstidt J. D. (1994) The kinetics and electrochemical rate-determining step of aqueous pyrite oxidation. *Geochim. Cosmochim. Acta* 58, 5443-5454.

Wogelius R. A. and Walther J. V. (1991) Olivine dissolution at 25°C: Effects of pH, CO_2, and organic acids. *Geochim. Cosmochim. Acta* 55, 943-954.

Wogelius R. A. and Walther J. V. (1992) Olivine dissolution kinetics at near-surface conditions. *Chem. Geol.* 97, 101-112.

Wood B. J. and Walther J. V. (1983) Rates of hydrothermal reactions. *Science* 222, 413-415.

Xiao Y. and Lasaga A. C. (1994) Ab initio quantum mechanical studies of the kinetics and mechanisms of silicate dissolution: H^+ (H_3O^+) catalysis. *Geochim. Cosmochim. Acta* 58, 5379-5400.

Xiao Y. and Lasaga A. C. (1996) Ab initio quantum mechanical studies of the kinetics and mechanisms of quartz dissolution: OH^- catalysis. *Geochim. Cosmochim. Acta* 60, 2283-2295.

Xiao Z., Jonckbloedt R. C. L., and Schuiling R. D. (1999) Neutralization of waste acids with olivine-dissolution in organically contaminated acids. *Chemie de Erde* 59, 33-45.

Zhang H. and Bloom P. R. (1999) Dissolution of hornblende in organic acid solutions. *Soil Sci. Soc. Am. J.* 63, 815-822.

Zhang J. W. and Nancollas G. H. (1990) Mechanisms of growth and dissolution of sparingly soluble salts. In *Mineral-Water Interface Geochemistry* (eds. M. F. Hochella, Jr. and A. F. White). Mineralogical Society of America, Washington, D.C. pp. 365-396.

Zhang Y. and Dawe R. (1998) The kinetics of calcite precipitation from high salinity water. *Appl. Geochem.* 13, 177-184.

Zhang Y. and Dawe R. A. (2000) Influence of Mg^{2+} on the kinetics of calcite precipitation and calcite crystal morphology. *Chem. Geol.* 163, 129-138.

Zhong S. and Mucci A. (1989) Calcite and aragonite precipitation from seawater solutions of various salinities; precipitation rates and overgrowth compositions. *Chem. Geol.* 78, 283-299.

Zhong S. and Mucci A. (1993) Calcite precipitation in seawater using a constant addition technique: A new overall reaction kinetic expression. *Geochim. Cosmochim. Acta* 57, 1409-1417.

Zuddas P. and Mucci A. (1994) Kinetics of calcite precipitation from seawater: I. A classical chemical kinetics description for strong electrolyte solutions. *Geochim. Cosmochim. Acta* 58, 4353-4362.

Zuddas P. and Mucci A. (1998) Kinetics of calcite precipitation from seawater: II. The influence of the ionic strength. *Geochim. Cosmochim. Acta* 62, 757-766.

Zysset M. and Schindler P. W. (1996) The proton promoted dissolution of K-montmorillonite. *Geochim. Cosmochim. Acta* 60, 921-931.